A Case Study on Environmental Design Methods toward the Lifecycle Carbon Reduction of Residential Buildings in Severe Cold Regions in China

中国における寒冷地住宅の脱炭素化に向けた環境設計手法に関する事例研究

楊 涵/Yang Han

2024 年 05 月

Catalogue

1.Introduction

1.1. Research Background

Measures aimed at significantly reducing global greenhouse gas emissions, limiting the increase in global temperatures to 2°C in this century, and striving to limit temperature increases to 1.5°C, were proposed under the 2015 Paris Agreement[1].

To try to limit temperature rise to 1.5°C, global greenhouse gas emissions would have to fall by an estimated 7.6% per year from 2020 to 2030 estimated at 12-15 billion tons. Limiting the temperature increase to 2°C would require an annual decline of 2.7% estimated at 29-32 billion tons of CO_2. The annual aberration in global mean surface temperature (i.e., the average of land-based near-surface air temperature and SST) in 2022 is 0.24°C above the 1991-2020 mean (0.79°C above the 20th century mean), This is the sixth warmest year since 1891. On longer time scales, the global mean surface temperature increases at a rate of about 0.74°C per century[2]. The global average surface temperature from 1870 to 2022 is shown in Figure 1.

According to data from the Global Carbon Project, China's carbon dioxide emissions in 2018 were 10.1 billion tons, ranking first in the world, accounting for 27.6% of global carbon dioxide emissions[3]. According to the "China Building Energy Research Report (2020)", Chinese carbon dioxide emissions climbed by 6.6 percent every year from 2005 to 2018, rising from 2.234 billion tons in 2005 to 4.932 billion tons in 2018. Figure 2 illustrates this. In September 2020, China announced that it would peak carbon dioxide emissions by 2030 and achieve carbon neutrality by 2060. In order to achieve the proposed goals, it is imperative for China's various industries to reduce carbon emissions[4]. According to the 2022 China Building Energy Consumption and Carbon Emissions Research Report, the total carbon emissions of the lifecycle building in China in 2020 was 5.08 billion tCO_2, accounting for 50.9% of the total carbon emissions[5].

China's construction market is huge, accounting for about 40% of the world's total construction volume[6]. Although the growth rate of China's energy demand has slowed down significantly, China will still be the world's largest energy consumer by 2040, accounting for 22% of global energy consumption[7]. Therefore, designing buildings to reduce emissions is an important part of achieving building decarbonization.

China's current total construction area reaches 56 billion square meters, of which about 60% are residential buildings[8]. Therefore, residential building emission reduction is an important measure to achieve China's carbon emission targets. In 2022, data from the China Building Energy Consumption and Carbon Emissions Research Report show that carbon emissions from building materials production are generally on an upward trend, rising from 1.09 billion tCO_2 in 2005 to 2.82 billion tCO_2 in 2020, with an average annual growth rate of 6.5%[9]. In 2018, carbon emissions from China's construction operations were approximately 2.1 billion tons, accounting for approximately 20% of total social emissions[10]. Among them, heating energy in northern cities and towns consumes 212 million tons of standard coal, and carbon emissions are about 550 million tons. Throughout 2022, cooling and heating demand from extreme weather pushed up global emissions by around 60 Mt CO_2, around two-thirds of which came from additional cooling needs, and the remaining third from heating needs[11]. This accounted for almost one-fifth of the total global increase in CO_2 emissions. However, due to China's vast geographical span, the dominant influencing factors of building carbon dioxide emissions are closely related to climate and environment[12]. Winter temperatures in China's severe cold regions are low, and heating is needed to maintain indoor temperatures at standard values. However, heating will cause carbon emissions in severely cold regions to be significantly higher than in other areas. Therefore, this article studies a design method based on carbon dioxide reduction, aiming to provide new ideas for the life cycle emission reduction of residential buildings in severe cold regions.

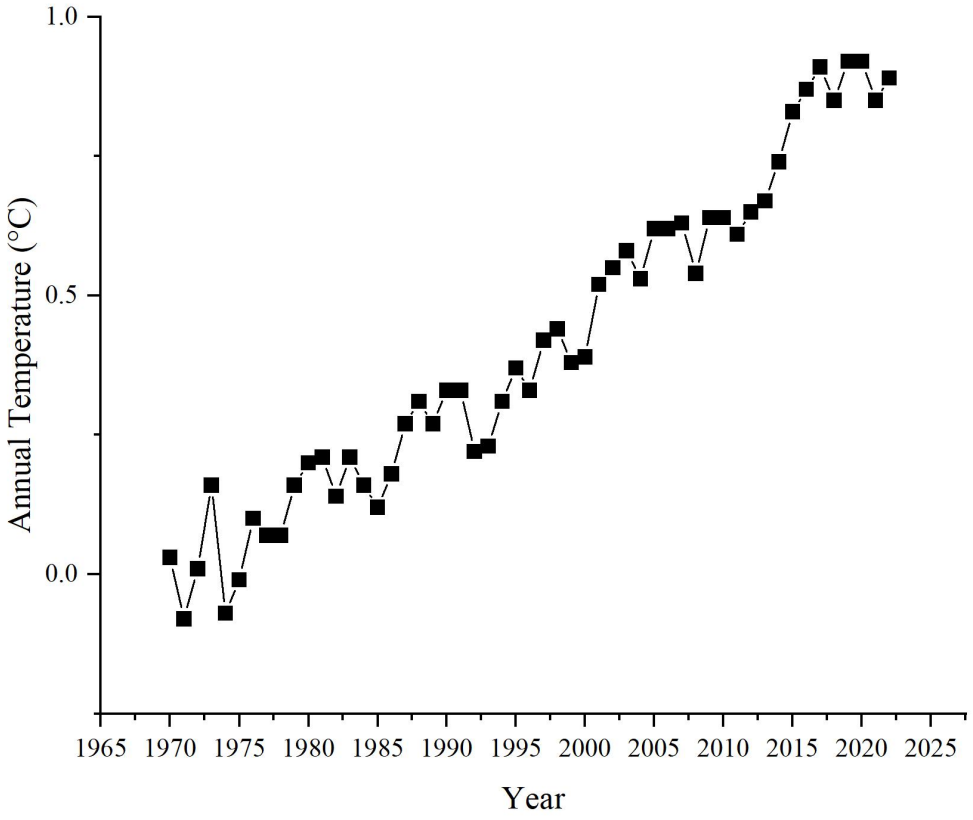

Figure 1. Global average surface temperature map from 1870 to 2022.

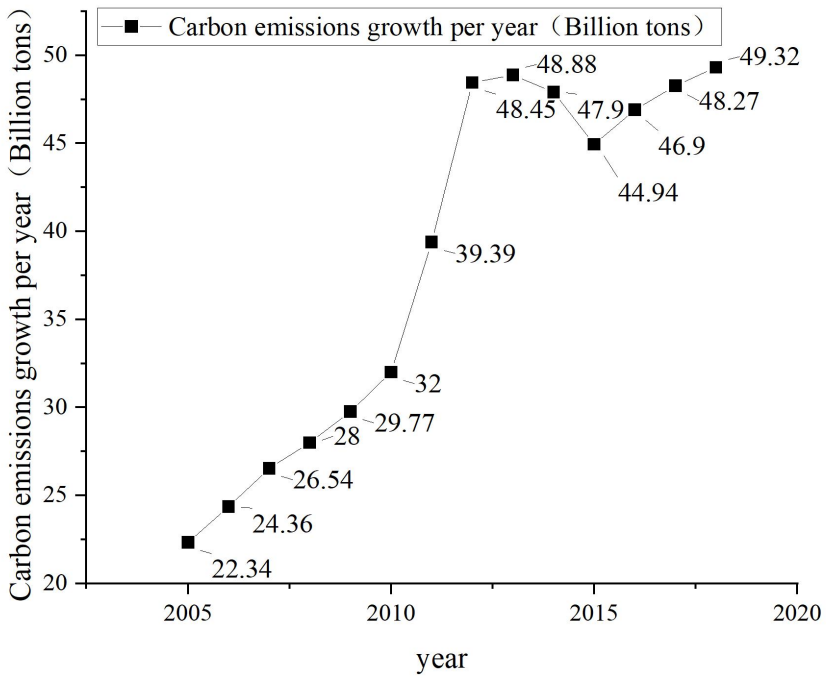

Figure 2. Growth of carbon emissions in China from 2005 to 2018.

1.2. Research Status

Since the Paris Agreement in 2005, which raised the serious CO_2 emission problem faced by the society nowadays, we have begun to carry out gradual explorations on the reduction of CO_2 emissions from buildings[13].

1.2.1. Status of Research in China

China as early as in the late 1980s began to vigorously promote building energy efficiency[14]. In 1986, proposed that the northern residential building energy consumption should be in 1980 to 1981 on the basis of building energy consumption to improve energy efficiency 30%[15]. 1993 proposed a further 30% increase in energy efficiency on the basis of the original, that is to say, than just advocate building energy efficiency when the building energy consumption based on energy efficiency 50%. Due to the 21st century before building energy efficiency in China has not been popularized so China's buildings are basically non-energy-efficient buildings[16]. Into the 21st century, China's building energy efficiency is gradually on track, the construction industry continues to high energy consumption, high carbon emissions pressure, so that the Government of China has gradually realized that the existing building emissions reduction and transformation is imperative.

"The Tenth Five-Year Plan strongly advocates the research and development of renewable energy sources such as solar energy and its application in energy-saving retrofit projects for existing buildings[17]. During the "Eleventh Five-Year Plan", it was made clear to increase the efforts to renovate the envelope structure, and to adopt heat metering charges for heat supply of existing buildings. "Twelfth Five-Year Plan" put forward: by 2015, the cumulative completion of the northern heating areas of existing residential building heating using heat measurement charges and energy-saving renovation of more than 400 million square meters of the binding target[18] . Due to the "12th Five-Year Plan" period of energy saving and emission reduction achieved remarkable results, so in the 12th Five-Year Plan policy and objectives based on the "13th Five-Year Plan" period to increase efforts to promote energy-saving renovation of existing residential buildings to achieve energy-saving renovation area of more than 500 million square meters of the target.

In recent years, many scholars have explored different aspects of residential building renovation. Li Jintang[19] analyzes the composition of heat consumption of buildings through the energy-saving renovation projects of typical existing residential buildings and agricultural houses in Luoyang City, and obtains the focus of energy-saving renovation for external walls, windows and roofs; He Zhangze[20]concludes that the influencing factors of energy consumption of the buildings in Hubei region in the order of heat transfer coefficients of external windows, external walls and roofs, and floor slabs. Wang Yilin[21] studied the application of molded polystyrene board, extruded polystyrene board, polyurethane foam board and graphite polystyrene board as the object of an existing residential building in Zhengzhou, the impact of energy-saving retrofit programs in different thickness of four types of thermal insulation materials on the energy consumption of the building and concluded that the choice of 40 mm polyurethane foam board for the external wall material is the optimal program. Ren Jingwei[22] took existing houses of different ages in Dalian City, a cold region, as an example, and concluded that from the perspective of heat consumption, the type of window glass has the greatest impact on energy consumption, followed by the roof, and finally the area of south-facing windows. Scholars have contributed important research data to the energy-saving retrofit of existing buildings in China through continuous experimental exploration.

Although the proposal of China's residential building design program has made remarkable achievements in residential building emission reduction, the situation of carbon dioxide emissions from residential buildings is still serious, and the discrepancy between the expected effect of design and the actual results of some projects, and the model not adapted to the regional situation leading to the failure of the design effect to be fully utilized and other problems have always existed.

1.2.2. Status of Foreign Research

Foreign building energy conservation work was carried out earlier, and the country has established a relatively complete system of policies and regulations to promote energy-saving renovation of buildings.

In Japan, the Ministry of Land, Infrastructure, Transportation and Tourism issued the "green hall social benchmark" in 1999, and the standard of green building was introduced for the first time. In 2008, the evaluation of simple through the application of CASBEE was started[23]. After continuous time exploration, the LCCM residential accreditation system was implemented in 2011[24]. In 2020, the Japanese government announced the goal of realizing a decarbonized society by 2050 due to the influence of the world environment[25]. As a result of the goal, research on carbon reduction in the construction industry was put on the agenda. After continuous exploration, it has been found that buildings generate a large amount of carbon dioxide in the early stages of construction and account for a large proportion of total building emissions, and also generate a large amount of carbon dioxide during operation and maintenance, so energy saving and emission reduction should be carried out in the whole life cycle of buildings.

France introduced its first building energy efficiency code in 1974 and continued to improve energy efficiency standards for 31 years until 2005[26]. The promulgation of the "Implementation Program for Climate Change Countermeasures" in 2004 stipulated that building energy-saving standards will be updated every five years, which pushed France's energy-saving renovation to a new stage of development. Because of continued improvements in energy efficiency standards, energy consumption for residential heating increased by only 3% in France between 1973 and 2002, despite a 70% increase in total residential floor space. However, the current situation of energy consumption in existing residential buildings is still very serious. The energy consumption of existing residential buildings accounts for 40% of the total energy consumption in the country. In order to mobilize the public's enthusiasm for energy-saving renovation of existing residential buildings, the French government provides financial subsidies to the public: if the homeowner If the energy consumed is 8% to 15% lower than the French average energy consumption standard, 50% of the house and land tax can be reduced[27].

The UK has vigorously pursued the exploration of clean energy, among which solar energy has achieved the most significant results. Through the government's exploration of solar energy, a passive solar house came into being that uses building insulation materials as a medium and does not require external machinery to be involved in operation. It is based on the principle of natural exchange of hot and cold air[28]. Due to the utilization of solar energy, the total energy consumption of the renovated building is reduced by 30%, achieving the effect of building energy saving. Therefore, passive solar houses are widely promoted.

Due to the government's vigorous promotion, foreign scholars have also carried out different explorations and research on the energy-saving retrofit of existing buildings. Kaynakli et al[29] compared and optimized the thickness of building thermal insulation in four regions of Turkey by considering the effect of the use of solar radiation on the annual energy demand of the building. Ucar A et al[30] proposed three different methods for determining the optimal thickness of building thermal insulation for the retrofit of existing buildings. The first method is based on the life cycle cost of energy consumption. The second method is a thermo-economic optimization based on the cost of insulation materials. The third method is to optimize the thickness of the insulation layer based on the thermal energy demand of the building using the Turkish Thermal Insulation Standard TS82. The results showed that the optimal thickness of the insulation was 3.2-12 cm, the energy savings ranged from 2.63 to 4.35 USD/㎡, and the payback period was 1.7-2.7 years, and the thickness depended on the region and the optimization method. Ashouri M et al.[31] optimized the thickness of the insulation of the walls of a building by using a combination of comparative analysis and life-cycle evaluation Rock wool and Glass wool for a detailed comparative analysis. Sisman N et al[32] Optimization of the thickness of external wall and roof insulation for an existing building based on energy consumption and economic cost. Carletti et al[34] Simulation of energy consumption through the EnergyPlus dynamic simulation system using an Italian building as a model. The replacement of existing windows with high energy performance windows, as well as the introduction of shading devices and solar control glazing, resulted in a reduction of the energy consumption of the existing building. Cascone S et al[34] selected different green roof options in Catania to be evaluated and compared their performance with the results of previous studies. The results showed that in terms of energy savings, cooling energy consumption was reduced by 31-35% and winter heating energy consumption

by 2-10%. Berardinis P.D et al[35] used double glazing envelope versus glazing envelope for retrofitting of existing buildings in Italy, and the comparison showed that the double-glazing envelope was more energy efficient.

1.3. Purpose of the Study and Significance of the Study

1.3.1. Research Purpose

Since China has a wide geographical span and the main influencing factors of building carbon dioxide emissions are closely related to the climate environment, the degree of promotion of residential emission reduction is also different in various regions. Therefore, residential emission reduction renovation presents complexity. This article aims to obtain the best design solution for residential emission reduction in severe cold regions through simulation analysis. By using Design Builder modeling software, a virtual residential building model was constructed, and the models were placed in three locations in Changchun City, Jilin Province, Shenyang City, Liaoning Province, and Datong City, Shanxi Province, in severe cold regions, and the annual carbon emissions were measured respectively. Taking the temperature changes, building structure changes, and external structural performance changes in the past 20 years as the main variable parameters, the emission reduction data of the building under the new plan was obtained based on simulation and the emission reduction design plan of residential buildings in severe cold regions was optimized, aiming to provide It provides new ideas for the whole life cycle emission reduction of residential buildings in severe cold regions.

1.3.2. Research Significance

At present, China is still in the active exploration stage for building carbon dioxide emission reduction plans. However, it is urgent to achieve the peak of carbon dioxide emissions before 2030 and to achieve carbon neutrality before 2060[36]. Therefore, many experimental attempts are now needed as a basis to accelerate the improvement of building carbon dioxide emissions. Determination of emission reduction plans and implementation of measures.

Among them, the carbon dioxide emissions caused by heating in severe cold regions cannot be ignored[37][38][39][40][41]. Coupled with the increasing extreme weather year by year, the carbon dioxide emissions in severe cold

regions increase year by year. Therefore, this article analyzes the specific impact of temperature changes on carbon dioxide emissions in severe cold regions. A detailed simulation was carried out, and the temperature changes in three severely cold cities in Changchun City of Jilin Province, Shenyang City of Liaoning Province, and Datong City of Shanxi Province in the past 20 years were selected as variables to simulate the spring, summer, autumn, winter and annual average temperature changes in various places. The impact on carbon dioxide emissions clearly demonstrates the impact of each quarter's temperature changes on building carbon emissions in severe cold regions.

According to data from the China Building Energy Consumption and Carbon Emissions Research Report in 2022, carbon emissions from building materials production are generally on an upward trend, rising from 1.09 billion tCO_2 in 2005 to 2.82 billion tCO_2 in 2020, with an average annual growth rate of 6.5%. Building materials will also cause huge carbon dioxide emissions not only in the production stage, but also in the building use stage, and different building materials have different impacts on the carbon dioxide produced in the building use stage[42]. Since trees have the ability to collect and fix carbon dioxide during their growth, consider replacing cement and steel bars with wood as building materials[43][44][45][46][47][48][49]. Replace reinforced concrete structures with timber-based buildings.

Therefore, this article attempts to simulate the specific impact of the two structures on carbon dioxide emissions in severe cold regions. At the same time, because the thermal performance of the building envelope is a key factor affecting the carbon emissions of residential buildings in severe cold regions, the heat loss through the building envelope accounts for 70% to 80% of the heat loss of the building[50]. According to calculations, the heat transfer coefficients of exterior walls, exterior windows, roofs, and other enclosure structures of residential buildings in severe cold regions in China are 3-5 times that of developed countries at the same latitude. Therefore, this article selects exterior windows, exterior walls, and roofs as architectural design parameter variables in severe cold regions. Through separate analysis and multi-factor analysis of exterior walls, roofs, and exterior windows, it clearly and specifically displays the relationship between exterior walls, roofs, and exterior windows in severe cold regions. Impact of carbon dioxide emissions. Through the exploration in the above three directions, we can not only clearly understand the current status of carbon dioxide emission reduction design in

severe cold regions, but also provide an important theoretical basis for the selection of architectural design solutions in severe cold regions.

1.4. Research Methodology

The main research methods used in this article are:

(1) Literature research

Find relevant literature on residential building energy conservation and emission reduction, read it carefully, and think repeatedly about the research path, research methods, and technical paths for research purposes. Finally, the research framework and research ideas of this article were formed.

(2) Investigation and research

During this research process, to have a comprehensive understanding of the exterior walls, windows, and roof renovation plans of existing residential buildings, we did a lot of work through extensive research and investigation.

During this survey, to fully understand the design of exterior walls, windows, and roofs of residential buildings in severe cold regions, we determined the corresponding design standards for residential buildings in severe cold regions by extensively reviewing information and checking the design standards of existing residential buildings. Standard codes and drawings.

Design parameters for residential buildings in severe cold regions are determined through extensive research, standard specifications and drawings.

(3) Simulation analysis method

Use Design Builder software to build a residential building model for carbon emission simulation.

(4) Comparative analysis

Using temperature changes, building structure changes, and thermal performance changes of envelope structures in the past 20 years as variables, the impact of changes in variables on carbon dioxide emissions from residential buildings in severe cold regions was studied.

1.5. Chapter Introduction

This article selects residential buildings in severe cold regions as the research object. It takes the building structure changes, and external structural performance changes in the severe cold regions as the main variable parameters, and conducts research based on the landforms and climate characteristics of the severe cold regions.

The main contents of the research are as follows:

Chapter 1 explains the research background, purpose and signifificance of the paper. At the same time, the research methods and technical routes of the paper are clearly given.

Chapter 2 explains the selection of simulation software and formulas and the analysis methods used.

This paper briefly explains the reasons for choosing DesignBuilder software for carbon emission simulation and introduces the data models involved later. It also introduces the calculation method of climate change tendency rate and the application of orthogonal analysis method.

Chapter 3 introduces the project overview and sets the model parameters based on the selection of residential buildings for model construction. And conduct carbon emission simulations for the building in three selected regions.

Chapter 4 describes the impact of temperature changes on carbon dioxide emissions over the past 20 years.

This chapter selects three cities in severe cold regions: Changchun City in Jilin Province, Shenyang City in Liaoning Province, and Datong City in Shanxi Province. Based on data from NASA Goddard Earth Science, we analyzed the average temperatures in Changchun, Shenyang, and Datongover the past 20 years, as well as the average temperatures in spring, summer, and winter. Based on the temperature data of various places in the past 20 years, DesignBuilder software was used to conduct carbon dioxide simulations to compare the impact of temperature changes in the past 20 years on spring, summer, autumn, winter and annual carbon dioxide emissions.

Chapter 5 describes the impact of changes in building structure on carbon dioxide emissions throughout the building's life cycle.

This chapter selects the original building structure - reinforced concrete structure and the new building structure - wooden structure to compare the carbon dioxide emissions in the entire life cycle and uses the inventory analysis method to analyze the material production stage, material transportation stage, building construction stage, and building operation throughout the building life cycle. During the building disassembly stage, carbon dioxide emissions are calculated, and the carbon dioxide emission reduction rates are compared.

Chapter 6 describes the impact of changes in building envelope on building carbon dioxide emissions.

This chapter studies the impact of changes on building carbon dioxide emissions from three aspects: exterior walls, roofs, and exterior windows. Analyze the impact of individual changes in exterior walls on building carbon dioxide emissions in severe cold regions, the impact of individual changes in exterior windows on building carbon dioxide emissions in severe cold regions, and the impact of individual changes in roofs on building carbon dioxide emissions in severe cold regions. DesignBuilder software was used to simulate the impact of simultaneous changes in the three factors of exterior walls, exterior windows, and roofs on building carbon dioxide emissions, and the optimal design plans for Changchun, Shenyang, and Datong were selected based on the orthogonal analysis method.

Chapter 7, Summary and Prospect.

2.Research Applications and Computational Model

Commonly used building simulation software now include DeST, PKPM, TRNSYS, OpenStudio, eQuest, DesignBuilder, etc. This article chooses DesignBuilder energy consumption simulation software to simulate building carbon emissions.

2.1. DesignBuilder Software

DesignBuilder is a comprehensive user graphical interface simulation software developed for a dynamic simulation program for building energy consumption (EnergyPlus). EnergyPlus, the powerful simulation engine for analyzing building energy consumption, can be used to simulate heating, cooling, ventilation and other energy consumption and carbon emissions in buildings. Different EnergyPlus simulators are available, including DOE2, DLL libraries, or any other available DOE program, which solves the problem of having a single simulator for most energy software. designBuilder includes the latest ASHRAE (American Society of Heating, Refrigeration and Air Conditioning) World Meteorological Data and Observations and provides free access to more than 2100 EnergyPlus hourly meteorological files. EnergyPlus time-of-day weather files are available free of charge, allowing instant simulation of a building's energy consumption under current conditions based on time-of-day weather data. The time step of the simulation results can be displayed in years, months, days, hours, or even less than an hour. This greatly improves the accuracy and precision of the simulation. Therefore, DesignBuilder is chosen as the carbon emission simulation software in this paper[51].

2.2. Computational Model

2.2.1. Computational Model for Reducing Carbon Dioxide Emission rate

Energy-saving efficiency is an index that evaluates the impact of parameters on building energy performance. Since this article needs to evaluate the impact of parameters on carbon oxide emissions from buildings in fifty years, this article chooses the rate of carbon dioxide emission reduction as the evaluation index[52]. The computational model of the carbon

dioxide emission rate is constructed as Equation (1).

$$RCDE=\frac{CDEPOP\text{-}CDEPMP}{CDEPMP}\times 100\% \quad (1)$$

Where *RCDE* is the reduce carbon dioxide efficiency, *CDEPMP* represents the building carbon dioxide emissions per year of a modify parameter plan, and *CDEPOP* represents the building carbon dioxide emissions per year of the original parameter plan.

2.2.2. Climate Change Trend Rate

Propensity rate is a commonly used expression when studying the changing trend of a certain feature quantity within a certain period[53].

Let *X* represent a certain climate element with a sample size of *n*, and let *t* represent the corresponding year. A linear regression equation of one variable is obtained by fitting.

$$X = k_0 t + b(t = 1.2.3.4.5\cdots n) \quad (2)$$

In the formula, k_0 is the regression coefficient. This paper uses the least squares method to estimate and takes 10 times of k_0 (i.e. $10k_0$) as the climate tendency rate of meteorological elements.

2.2.3. Economic Indicators

Because economic indicators must assess the economic feasibility and intuitively determine the program's entire benefits, as a result, the static investment payback period and net present value are used as economic indicators in this article.

(1) Net Present Value.

The net present value refers to the difference between the net cash flow generated by the investment plan and the present value of the original investment after discounting the cost of funds as the discount rate[54]. For this article, the net present value is the difference between the total annual cost savings of residential buildings and the incremental cost of residential buildings during the building life cycle. The computational model of net present value is constructed as Equation (3).

$$NPV = \sum_{t=1}^{n} (CI - CO)(1+i)^{-t} \qquad (3)$$

Where net present value is net present value in *USD*, *CI* represents annual savings after design transformation in *USD*, *CO* represents the difference between initial investment cost before design transformation and after design transformation in *USD*, *t* represents calculation year in years, *i* represents social discount rate.

There are two main types of calculation costs for this indicator: the annual cost savings after the design change and the difference between the initial investment costs before and after the design change.

A. Annual cost savings after design changes.

Annual cost savings following design changes should include energy savings and carbon trading fees[55]. The computational model is Equation (4). After the architectural design changes, the annual energy consumption of the building is reduced. Therefore, the number of raw materials for energy supply (calculated by coal) is reduced, thereby saving costs. After the design and renovation, the carbon emissions generated by residential buildings are reduced, and transactions can be carried out according to trading market to save costs. The computational model is constructed as Equations (5) and (6).

$$CI = C_1 + C_2 \qquad (4)$$

$$C_1 = \frac{E \times 3600 \times 24 \times 120}{\theta \times 10^6 \times \eta} \times F \qquad (5)$$

$$C_2 = T \times F_c \qquad (6)$$

Where C_1 represents the coal-saving cost after the design change in *USD*, C_2 represents the carbon trading fee after the design change in *USD*. E Represents the total energy consumption saved by the change plan in megawatt hours in *MWh*. F represents the market price of standard coal in *USD*. θ represents the calorific value of standard coal. η represents combustion efficiency of heating and combustion in *kJ/kg*. T Indicates the total carbon emissions saved by the change program in *kg*. Fc represents Carbon trading price in *USD*.

B. The initial investment cost difference before design transformation and after design transformation.

The difference between the initial investment cost before the design change and after the design binding includes costs for insulation materials, labor, machinery, etc. This article mainly calculates costs based on the 2019 version of the construction project pricing budget quota. Use Glodon's pricing software to calculate energy-saving renovation costs.

(2) Static Payback Period.

The static payback period is the time required for the project's net income to recover its entire investment[56]. For this article, the static payback period is the time during which the annual cost savings after the residential building renovation are equal to the incremental cost of the residential building renovation.

(3) Discounted Payback Period.

The discounted payback period is the total time required to offset the present value of the original investment with the present value of the net cash

flow of the investment project, considering the time value of money[57]. The computational model of net present value is constructed as Equation (7).

$$P_t = (N_1 - 1) + \frac{C_3}{C_4} \qquad (7)$$

Pt represents the discounted payback period in years. N_1 indicates the year in which the cumulative net cash flow is positive in *years*, and C_3 represents the absolute value of the present value of the cumulative net cash flow in the previous year in *USD*. C_4 indicates the present value of the net cash flow in the year in which the positive value occurs in *USD*.

2.3. Orthogonal Analysis

Orthogonal experimental design is a design method for studying multi-factor and multi-level. It selects some representative points from the comprehensive experiment based on orthogonality for testing[58]. These representative points have the characteristics of "evenly dispersed, neat and comparable". Orthogonal experimental design method: Based on Galois theory, a scientific experimental design method is used to select an appropriate number of representative points from a large amount of experimental data to rationally arrange the experiment. At present, orthogonal experiment design no longer requires searching for orthogonal tables before conducting experiments. For complex situations, orthogonal experiment software can now be used for experimental design.

Commonly used analysis methods in the orthogonal experimental method include visual analysis and variance analysis. The intuitive analysis method lists the analysis results more simply and intuitively, and the amount of analysis is small, but it cannot calculate the experimental error. The variance analysis rule can more accurately and quantitatively calculate the importance of factors. To analyze the data more rigorously, this article uses the intuitive analysis method and the variance analysis method to jointly conduct orthogonal test simulation results.

The intuitive analysis method mainly determines the primary and secondary degree of influence of factors on the test results based on the range

between various factors. The larger the range, the greater the impact of this factor on the test results. The average value is used to reflect the impact of different levels of the same factor on the test results, and to determine the optimal level of the factor.

The analysis of variance method mainly calculates the F value and P value. Use the P value to determine the degree of influence of factors on the experimental results. If $P > 0.05$, if $0.01 \leq P \leq 0.05$, the factor has a significant impact on the experimental results; if $P < 0.01$, the factor has an extremely significant impact on the experimental results. Use this to determine the main factors and secondary factors. According to the principle of variance analysis, you only need to choose the best level for the main factors, and for the secondary factors, you can choose the appropriate level according to the actual factors.

2.4. Summary of this Chapter

This chapter explains the choice of simulation software and formulas as well as the analysis methods used.

It briefly explains the reasons for choosing DesignBuilder software for carbon emission simulation and introduces the data models and concepts involved later. It also introduces the calculation method of climate change trend rate and the concept of orthogonal analysis method.

3.Modeling and Carbon Emission Simulation in China's Severe Cold Regions

3.1. Climatic Environment

The areas selected in this article are all severe cold regions (C). The zoning index of severe cold regions (C) is that the number of heating days is greater than 3800 and less than 5000. The locations of Changchun City in Jilin Province, Shenyang City in Liaoning Province, and Datong City in Shanxi Province are as shown in the Figure.3.

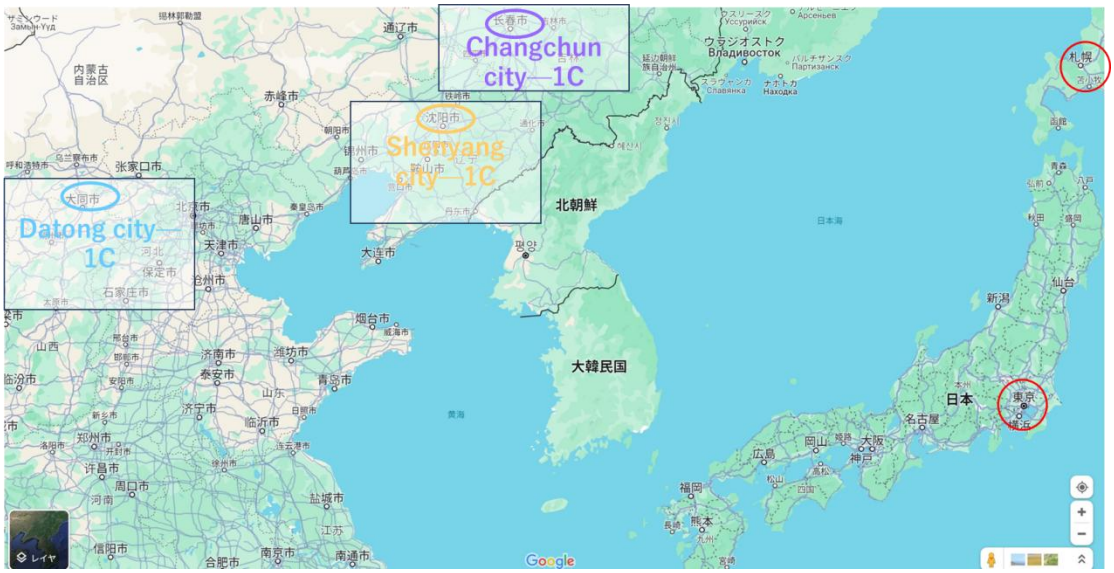

Figure 3. Changchun City, Shenyang City, Datong City Location

Changchun City is in the Songliao Plain in the hinterland of Northeast China, at 43°05′-45°15′ north latitude and 124°18′-127°05′ east longitude. The climate of Jilin Province is in the transition zone between the humid mountains in the east and the semi-arid plains in the west. It belongs to the temperate continental humid climate type. The annual average temperature is 4.6℃, the hottest monthly average temperature is 23℃, the maximum temperature is 40℃, the minimum temperature is -39.8℃, the sunshine time is 2688 hours, the annual precipitation is 600~700 *mm*, and the summer precipitation accounts for more than 60% of the annual precipitation. . The climate is characterized by dry and windy spring, short and hot and humid summer, sunny and large temperature difference in autumn, and long, dry and cold winter. The dominant wind direction is southwesterly all year round, and the dominant wind direction in winter is northwesterly. In autumn, sunny and warm weather can occur that lasts for several days, with larger temperature differences and lower wind speeds than in spring[59].

Shenyang City is in the southern part of Northeast China and the central part of Liaoning Province, between 41°48′11.75″ north latitude and 123°25′31.18″ east longitude. It has a temperate humid continental climate, with an average temperature of -10.9°C in January, an average temperature of 24.7°C in July, and an annual average temperature of 8.5°C. The annual precipitation in Shenyang City is 600~800*mm*. Affected by the monsoon, precipitation is concentrated in summer, the temperature difference is large, and the four seasons are distinct. The winter cold lasts for a long time, nearly six months[60].

Datong City is located at the northernmost tip of Shanxi Province, with east longitude 112°34′-114°33′ and north latitude 39°03′-40°44′. Datong City is located in the temperate continental monsoon climate zone. Affected by the monsoon, Datong has four distinct seasons. The temperature rises quickly in spring. The climate in Datong City is dry, cold and windy, with a large temperature difference. The annual average temperature is 6.4°C, and in January it was minus 11.8°C. The lowest temperature is minus 29.2℃, the average temperature in July is 21.9℃, and the annual precipitation is 400~500*mm*[61].

3.2. Model Overview

The model is a virtual model to construct a residential building with a total floor area of 2887.86 m² according to the architectural characteristics of cold regions. The first floor covers an area of 481.31 square meters. The number of floors of the building is 6 above grounds, all above ground, no underground construction. The floor height of 2.8m. The shape coefficient of 0.28.The building structure for reinforced concrete shear wall structure, the building wall for 370*mm* ordinary clay solid brick + 80*mm* EPS polystyrene foam board insulation materials, roof for reinforced concrete + 50*mm* EPS polystyrene foam board insulation materials. The external windows of the building are 4+10(A)+4 single silver Low-e+10(Ar)+4， Ordinary hollow glass plastic steel window. The simulation model established in Design Builder is shown in Figure 4.

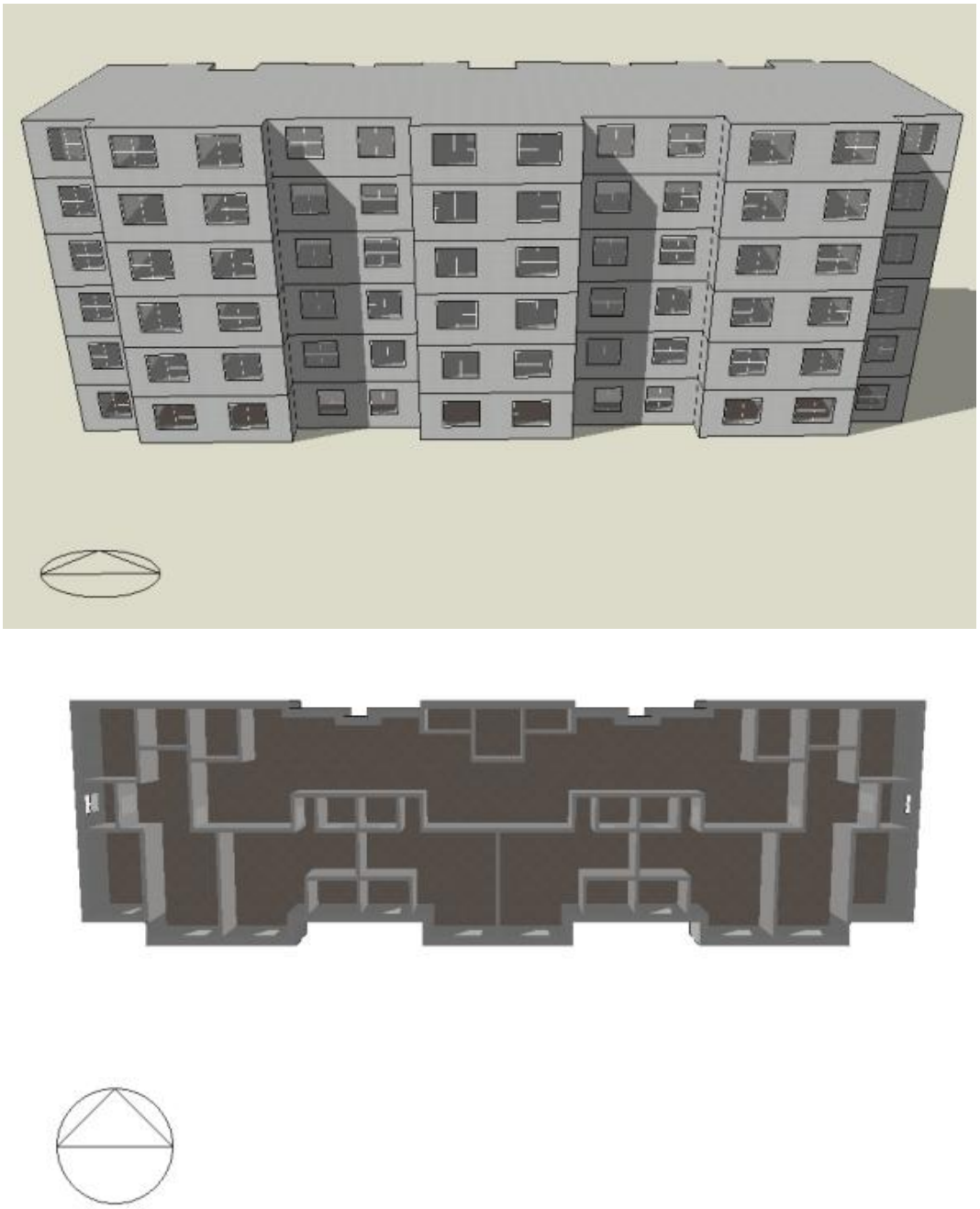

Figure 4. Simulation model of a residential building

According to Design standard for Energy Efficiency of Residential Buildings in severe cold and cold reigons[62], Changchun city, Shenyang city and Datong city belongs to the severe cold regions as defined by China, where the indoor temperature in winter is not lower than 18℃. In summer, the indoor temperature should not be higher than 26℃. The number of air exchanges calculated for winter heating should be 0.5 times/h. For places with lighting in the model, the power density of lighting is set at 5W/m^2 and the power density of equipment at 3.8W/m^2, and the personnel is set at two persons in the bedroom, three persons in the living room, and one person in other rooms. Shown in Table 1.

The heating method is centralized heating, and the fuel is coal. Cooling is air conditioning. Energy consumption is electricity.

3.3. Building Simulation of CO_2 Emissions Data

The weather parameters of the model will be set to the climate parameters of each region in 2022. The data used comes from NASA Goddard Earth Science. The annual carbon dioxide emissions of this building in Changchun City in 2022 are 118.7tCO_2, the annual carbon dioxide emissions of this building in Shenyang City in 2022 are 107.84tCO_2, and the annual carbon dioxide emissions of this building in Datong City in 2022 are 103.21tCO_2. According to data It can be seen that changes in temperature will indeed have an impact on building carbon dioxide emissions.

3.4. Summary of this Chapter

This chapter mainly establishes the architectural model in the Design Builder software and designs the building parameters according to the requirements of Zone C in severe cold regions according to the "Design Standards for Residential Buildings". At the same time, the climate and geographical environment of the three simulation areas selected in this article, Changchun City in Jilin Province, Shenyang City in Liaoning Province, and Datong City in Shanxi Province, were introduced. Annual carbon emissions were calculated based on the meteorological conditions of Changchun City, Shenyang City, and Datong City in 2022.

Table1. Original design parameters

Design Parameters	Data	Heat transfer coefficient
Exterior wall	25*mm* cement mortar+370*mm* hollow clay brick+60*mm*EPS polystyrene foam board+8*mm* cement mortar	0.4
Roof	40*mm* fine stone reinforced concrete+50*mm*EPS polystyrene foam board+1.2*mm* waterproof coiled material+20*mm* cement mortar leveling layer+30*mm* lightweight aggregate concrete slope finding+120*mm* reinforced concrete roof slab	0.2
Exterior window	4+10(A)+4 single silver Low-e+10（Ar）+4，Ordinary hollow glass plastic steel window	2.0
Floor height	2.8m	
Indoor temperature	not lower than 18℃、not higher than 26℃	
Air exchanges	0.5 times/h	
Power density of lighting	5W/m^2	
Power density of equipment	3.8W/m^2	
Personnel	two persons in the bedroom, three persons in the living room, and one person in other rooms.	
Heating method	centralized heating	
Cooling	air conditioning	
Window-to-wall ratio	North：0.20 East：0.25 South：0.30 West：0.25	

4.Impact of Temperature Changes on CO_2 Emissions Over the Past 20 Years

Based on climate observation data, using linear regression analysis method to study climate change is still one of the feasible and effective methods for climate change diagnosis. Therefore, this paper applies the linear regression method to analyze the changes in the average temperature and the average temperature in spring, summer, autumn and winter in Changchun City, Shenyang City and Datong City in the past 20 years.

4.1. Data Sources

The data areas required for this article are Changchun City in Jilin Province, Shenyang City in Liaoning Province, and Datong City in Shanxi Province. The data used comes from NASA Goddard Earth Science. The hourly average temperature data from 2002 to 2022 is selected to calculate the annual average temperature and the average temperature in spring, summer, autumn and winter.

4.2. Temporal Trends in Average Temperatures over the Last 20 Years

It can be seen from Figure 5 that the annual average temperature and the average spring, summer, autumn and winter temperature in Changchun City, Shenyang City, and Datong City in the past 20 years have shown an upward trend, and they have shown a multi-fluctuation trend.

It can be seen from Figure 5 that the annual average temperature trend rate in Changchun City shows an upward trend, with an average annual increase of 0.023°C. 2019 was the year with the highest annual average temperature, reaching about 7.6°C, and 2012 was the year with the lowest annual average temperature, which was about 5.2°C, the climate tendency rate of the annual average temperature change is 0.23℃/10a (passed the significance test of 0.05). The annual average temperature tendency rate of Shenyang City shows an upward trend, with an average annual increase of 0.023℃ and 2014 was the year with the highest annual average temperature, reaching about 10.3℃. 2012 was the year with the lowest annual average temperature, which was about 8.1℃. The climate tendency rate of annual average temperature change was 0.23℃/10a (passed the significance test of 0.05). The annual average temperature tendency rate of Datong City shows an upward trend, with an average annual increase of 0.027°C. 2007 was the year with the highest annual average temperature, reaching about 9.4°C and 2003 was the year with the lowest annual average temperature, reaching about 7.5°C. The climate tendency rate of the annual average temperature change was 0.27°C/ 10a (passed the significance test of 0.05).

As can be seen from Figure 6, the average spring temperature trend rate in Changchun City shows an upward trend, with an average annual increase of 0.038°C. 2008 was the year with the highest average spring temperature, reaching about 9.56°C, and 2013 was the year with the lowest average spring temperature, at about 5.72°C, the climate tendency rate of spring average temperature change is 0.38℃/10a (passed the significance test of 0.05). The average spring temperature trend rate in Shenyang City shows an upward trend, with an average annual increase of 0.044°C. 2002 was the year with the highest average spring temperature, reaching about 12.03°C. 2013 was the year with the lowest average spring temperature, reaching about 8.50°C. The average spring temperature changes the climate tendency rate is 0.44℃/10a (passed the significance test of 0.05). The average spring temperature trend rate in Datong City shows an upward trend, with an average annual increase

of 0.058°C. 2018 was the year with the highest average spring temperature, reaching about 10.28°C. 2010 was the year with the lowest average spring temperature, reaching about 5.93°C. Changes in the average spring temperature The climate tendency rate is 0.58℃/10a (passed the significance test of 0.05).

As can be seen from Figure 7, the average summer temperature trend rate in Changchun City shows an upward trend, with an average annual increase of 0.021°C. 2018 was the year with the highest average spring temperature, reaching about 23.30°C, and 2009 was the year with the lowest average summer temperature, at about 21.54°C, the climate tendency rate of summer average temperature change is 0.21℃/10a (passed the significance test of 0.05). The average summer temperature trend rate in Shenyang City shows an upward trend, with an average annual increase of 0.040°C. 2018 was the year with the highest average summer temperature, reaching about 25.24°C, and 2013 was the year with the lowest average summer temperature, reaching about 23.20°C. Changes in the average summer temperature The climate tendency rate is 0.40℃/10a (passed the significance test of 0.05). The average summer temperature trend rate in Datong City shows an upward trend, with an average annual increase of 0.016°C. 2018 was the year with the highest average summer temperature, reaching about 21.36°C. 2004 was the year with the lowest average summer temperature, reaching about 18.99°C. Changes in the average summer temperature The climate tendency rate is 0.16℃/10a (passed the significance test of 0.05).

It can be seen from Figure 8 that Changchun City's autumn average temperature trend rate shows an upward trend, with an average annual increase of 0.023°C. 2004 was the year with the highest average temperature in autumn, reaching about 8.55°C, and 2002 was the year with the lowest average temperature in autumn, at about 4.76°C. The climate tendency rate of summer average temperature change is 0.23℃/10a (passed the significance test of 0.05). The average autumn temperature trend rate in Shenyang City shows an upward trend, with an average annual increase of 0.012°C. 2004 was the year with the highest average temperature in autumn, reaching about 10.75°C, and 2002 was the year with the lowest average temperature in autumn, at about 7.61°C. The average temperature in autumn changes The climate tendency rate is 0.12℃/10a (passed the significance test of 0.05). Datong City's autumn average temperature trend rate shows an upward trend, with an average annual increase of 0.012°C. 2006 was the year with the

highest average temperature in autumn, reaching about 8.72°C. 2012 was the year with the lowest average temperature in autumn, at about 5.37°C. The average temperature changes in autumn the climate tendency rate is 0.12℃/10a (passed the significance test of 0.05).

As can be seen from Figure 9, Changchun City's average winter temperature tendency shows a slight downward trend, with an average annual decrease of 0.001°C. 2006 was the year with the highest average temperature in winter, reaching about -8.74°C, and 2012 was the year with the lowest average temperature in winter, which was around 18.05℃, the climate tendency rate of winter average temperature change is 0.01℃/10a (passed the significance test of 0.05). The average winter temperature tendency rate of Shenyang City shows an upward trend, with an average annual increase of 0.046°C. 2006 was the year with the highest average temperature in winter, reaching about -5.41°C. 2012 was the year with the lowest average temperature in winter, at about -10.51°C. The winter average the climate tendency rate of temperature change is 0.46℃/10a (passed the significance test of 0.05). Datong City's winter average temperature trend rate shows an upward trend, with an average annual increase of 0.054°C. 2016 was the year with the highest average temperature in winter, reaching about -5.96°C. 2011 was the year with the lowest average temperature in winter, at about -9.57°C. The winter average the climate tendency rate of temperature change is 0.54℃/10a (passed the significance test of 0.05).

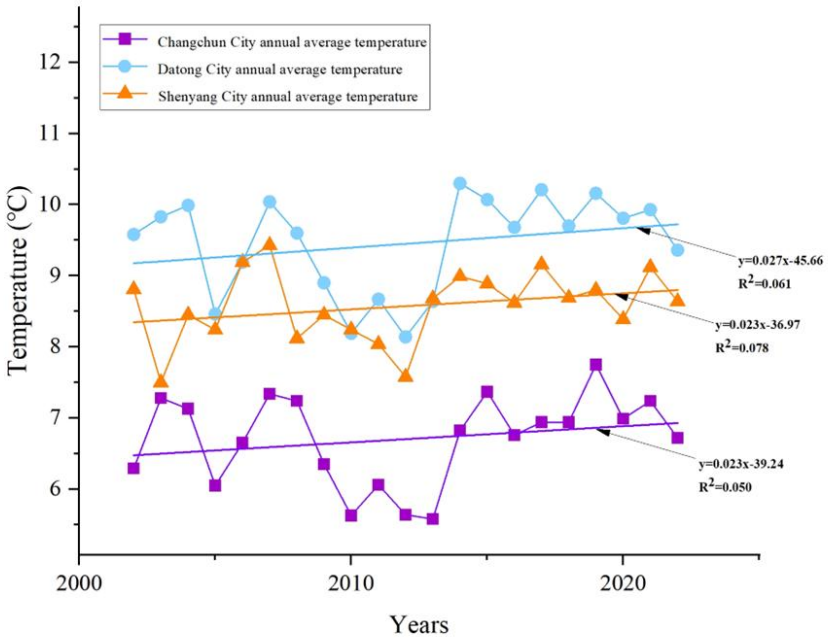

Figure 5. Changchun City, Shenyang City, Datong City 20-year average annual temperature

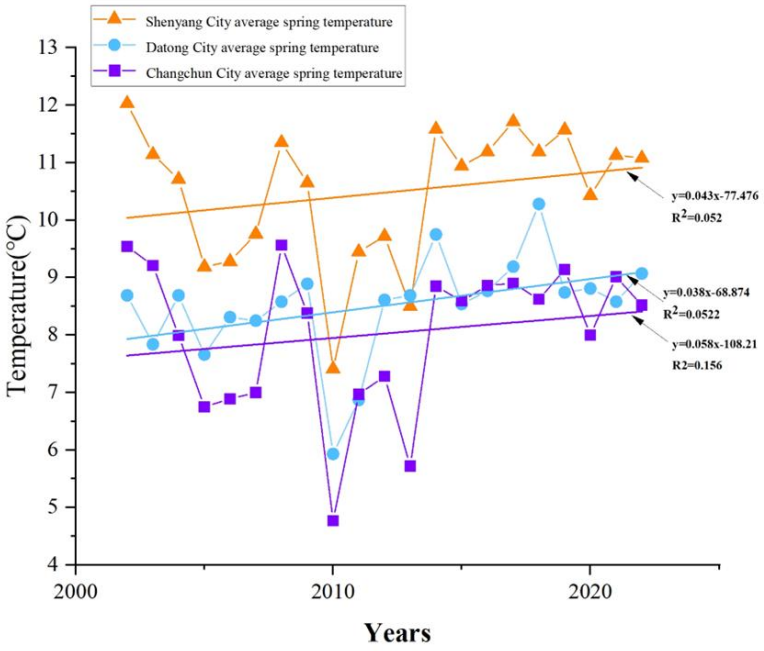

Figure 6. Changchun City, Shenyang City, Datong City 20-year average spring temperature

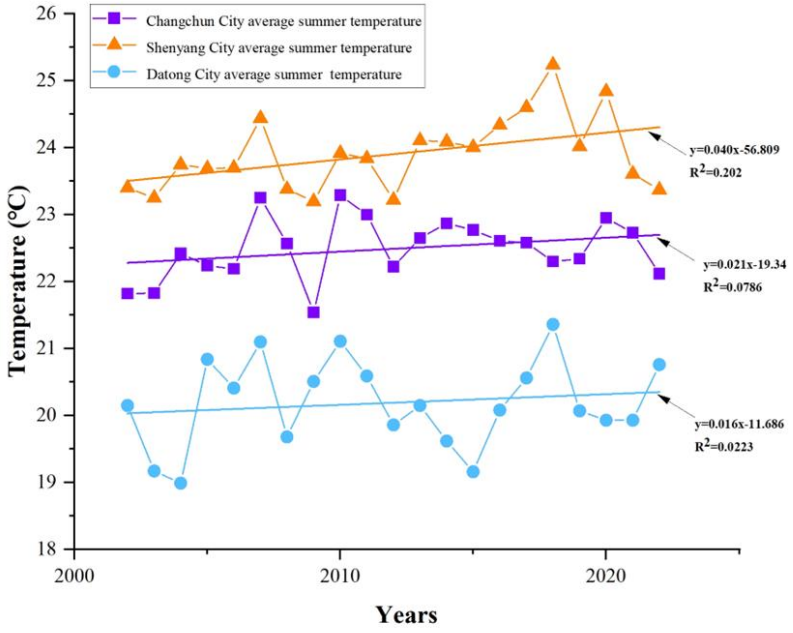

Figure 7. Changchun City, Shenyang City, Datong City 20-year average summer temperature

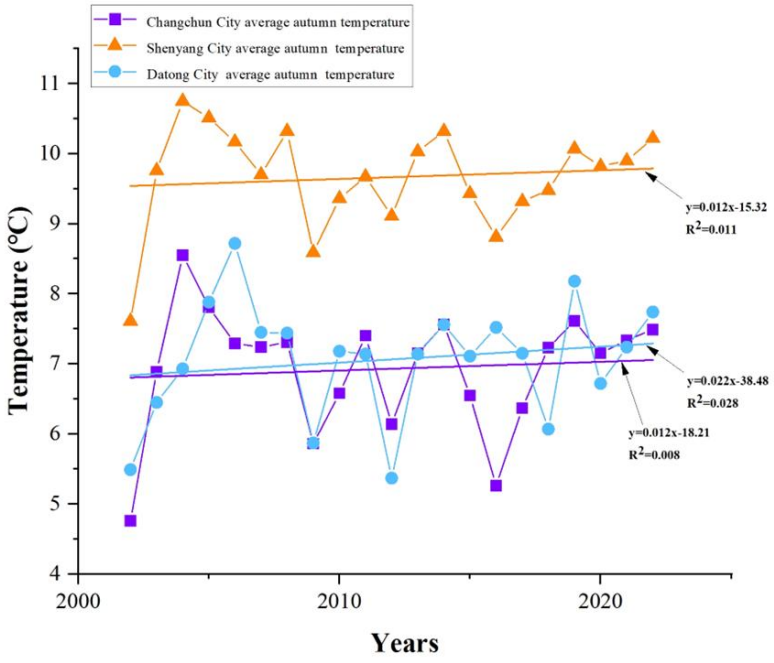

Figure 8. Changchun City, Shenyang City, Datong City 20-year average autumn temperature

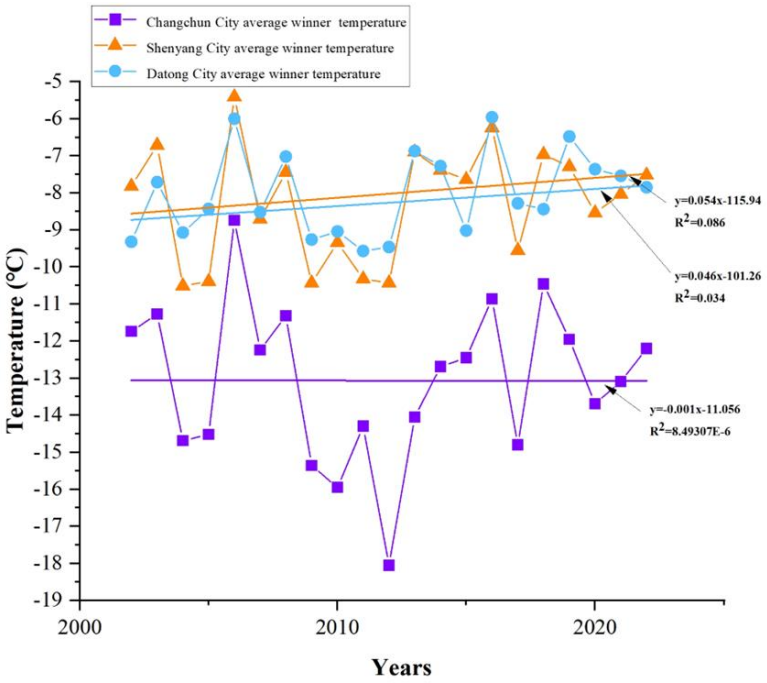

Figure 9. Changchun City, Shenyang City, Datong City 20-year average winter temperature

4.3. Simulation of Temperature Changes

Based on annual average temperature, spring, summer, autumn and winter average temperature data, carbon dioxide emissions as a function of temperature were simulated over the past 20 years. As shown in Figures 10-14.

As can be seen from Figure 10, the propensity rate of spring carbon dioxide emissions in Changchun City, Shenyang City, Datong City, exhibits an upward trend as the temperature changes. Among them, the spring carbon dioxide emissions in Changchun City rose by 0.17t, and 2020 was the highest year of annual carbon dioxide emissions, amounting to about 39.2t, and 2002 was the lowest year of spring carbon dioxide emissions, amounting to about 29.3t, with a propensity rate of spring carbon dioxide emissions of 1.7t/10a (passed the significance test of 0.05) . In Shenyang City, annual spring carbon dioxide emissions rose by 0.12t, and 2018 was the highest annual carbon

dioxide emissions year, amounting to about 109.6t, and 2014 was the lowest annual carbon dioxide emissions year, amounting to about 101.1t, with a propensity rate of spring carbon dioxide emissions of 1.2t/10a (passed the significance test of 0.05). The annual spring carbon dioxide emission in Datong City rises by 0.051t, 2022 is the highest annual carbon dioxide emission year, amounting to about 35.7t, and 2018 is the lowest annual carbon dioxide emission year, amounting to about 29.7t, with a propensity rate of spring carbon dioxide emission of 0.51t/10a (passing a significance test of 0.05) .

As can be seen from Figure 11, the propensity rate of summer carbon dioxide emissions in Changchun City, Shenyang City, Datong City, shows an increasing trend with the change of temperature. Among them, the summer carbon dioxide emissions in Changchun City rose by 0.01t, 2008 was the highest year of annual carbon dioxide emissions, amounting to about 14.8t, and 2019 was the lowest year of spring carbon dioxide emissions, amounting to about 12.7t, and the propensity rate of summer carbon dioxide emissions was 0.06t/10a (passed the significance test of 0.05) . Shenyang City annual summer carbon dioxide emissions rise 0.03t, 2018 is the highest year of annual carbon dioxide emissions, amounting to about 16.2t, 2004 is the lowest year of annual carbon dioxide emissions, amounting to about 13.8t, and the propensity rate of summer carbon dioxide emissions 0.28t/10a (passed the significance test of 0.05). The annual summer carbon dioxide emission in Datong City rises by 0.065t, and 2014 is the highest year of annual carbon dioxide emission, amounting to about 16.4t, and 2005 is the lowest year of annual carbon dioxide emission, amounting to about 13.2t, with a propensity rate of summer carbon dioxide emission of 0.65t/10a (passed the significance test of 0.05).

As can be seen from Figure 12, the propensity rate of autumn carbon dioxide emissions in Changchun City, Shenyang City, Datong City, exhibits an increasing trend with the change of temperature. Among them, the autumn carbon dioxide emissions in Changchun City rose by 0.03t, 2012 was the highest year of annual carbon dioxide emissions, amounting to about 20t, and 2017 was the lowest year of spring carbon dioxide emissions, amounting to about 18.4t, and the propensity rate of autumn carbon dioxide emissions was 0.3t/10a (passed the significance test of 0.05). Shenyang City annual autumn carbon dioxide emissions rise 0.018t, 2013 is the highest year of annual carbon dioxide emissions, amounting to about 18.4t, 2004 is the lowest

year of annual carbon dioxide emissions, amounting to about 17t, the tendency rate of autumn carbon dioxide emissions 0.18t/10a (passed the significance test of 0.05). The annual autumn CO_2 emission in Datong City rises by 0.005t, 2021 is the highest year of annual CO_2 emission, which reaches about 18.5t, and 2014 is the lowest year of annual CO_2 emission, which is about 17t, and the propensity rate of autumn CO_2 emission is 0.05t/10a (passed the significance test of 0.05).

As can be seen from Figure 13, the propensity rate of winter carbon dioxide emissions in Changchun City, Shenyang City, Datong City, shows an increasing trend with the change of temperature. Among them, the winter carbon dioxide emissions in Changchun City rose by 0.018t, and 2010 was the highest year of annual carbon dioxide emissions, amounting to about 45.2t, and 2002 was the lowest year of spring carbon dioxide emissions, amounting to about 43.2t, and the propensity rate of winter carbon dioxide emissions was 0.18t/10a (passed the significance test of 0.05). Shenyang City annual winter carbon dioxide emissions rise 0.087t, 2019 is the highest year of annual carbon dioxide emissions, amounting to about 43.6t, and 2003 is the lowest year of annual carbon dioxide emissions, amounting to about 40.2t, the propensity rate of winter carbon dioxide emissions 0.87t/10a (passed the significance test of 0.05). The annual winter CO_2 emission in Datong City rises by 0.29t, 2019 is the highest annual CO_2 emission year, amounting to about 43.9t, and 2007 is the lowest annual CO_2 emission year, amounting to about 40.2t, with a propensity rate of winter CO_2 emission of 2.9t/10a (passed the significance test of 0.05).

It can be seen from Figure 14 that as the temperature changes, the tendency rate of annual carbon dioxide emissions in Datong City, Shenyang City, Changchun City shows an upward trend. Among them, the average annual carbon dioxide emissions in Changchun City increased by 0.039t. 2021 was the year with the highest annual carbon dioxide emissions, reaching about 118.9t. 2004 was the year with the lowest annual carbon dioxide emissions, at about 106.6t. The tendency rate of annual carbon dioxide emissions was 0.38t/10a (passed the significance test of 0.05). The average annual carbon dioxide emissions in Shenyang increased by 0.28t. 2018 was the year with the highest annual carbon dioxide emissions, reaching about 109.6t. 2014 was the year with the lowest annual carbon dioxide emissions. It is about 101.1t, and the tendency rate of annual carbon dioxide emissions is 2.8t/10a (passed the significance test of 0.05). The average annual carbon dioxide

emissions in Datong City increased by 0.11t, and 2018 was the year with the highest annual carbon dioxide emissions, reaching 107.6 t, 2003 was the year with the lowest annual carbon dioxide emissions, which was about 96.2t, and the tendency rate of annual carbon dioxide emissions was 1.1t/10a (passed the significance test of 0.05).

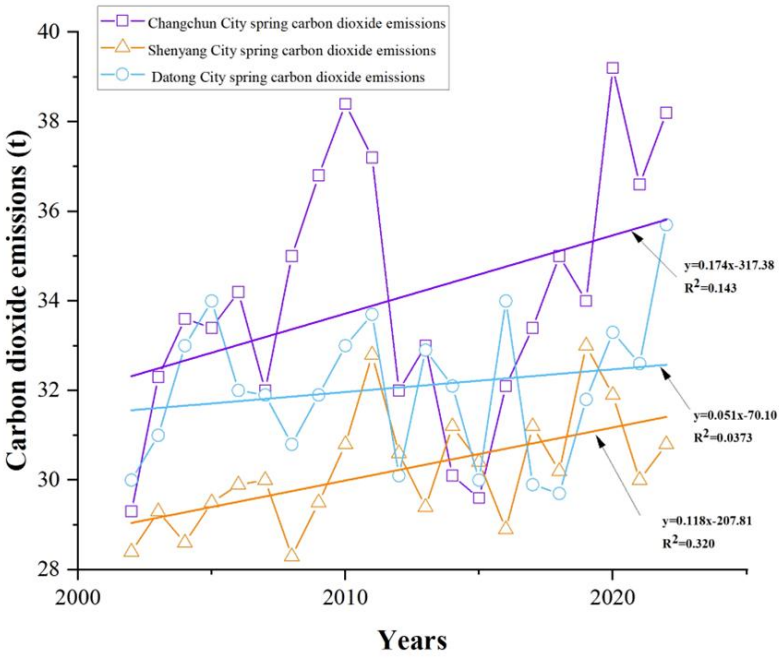

Figure 10. CO_2 emissions in the spring of Changchun City, Shenyang City, Datong City in the past 20 years

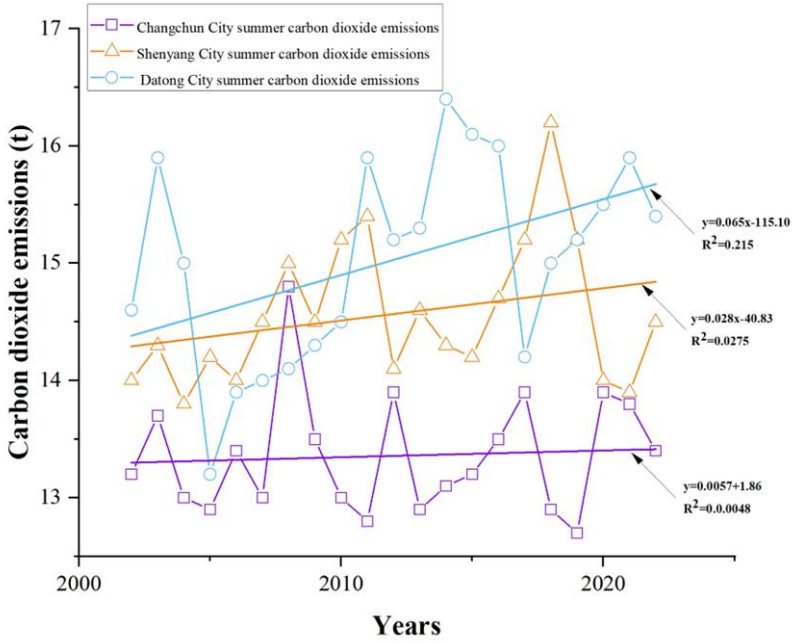

Figure 11. CO_2 emissions in the summer of Changchun City, Shenyang City, Datong City in the past 20 years

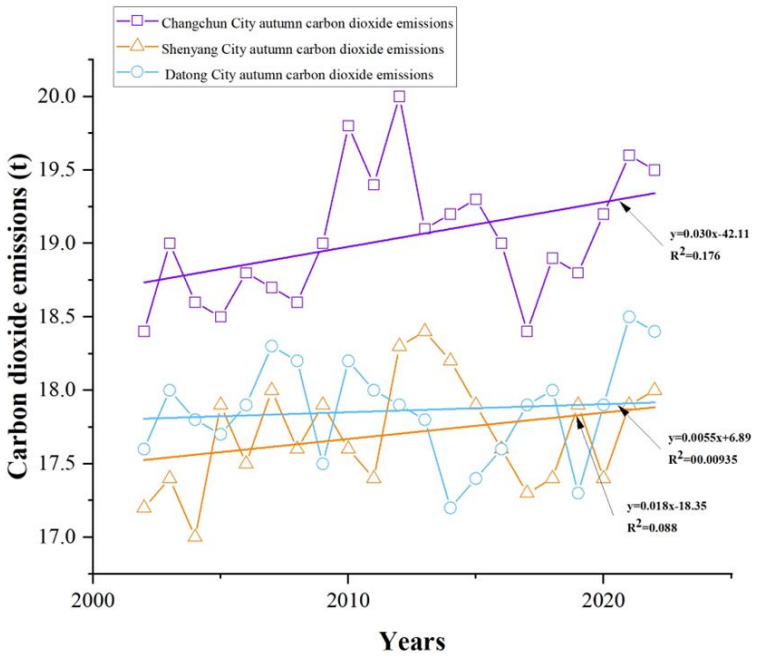

Figure 12. CO_2 emissions in the autumn of Changchun City, Shenyang City, Datong City in the past 20 years

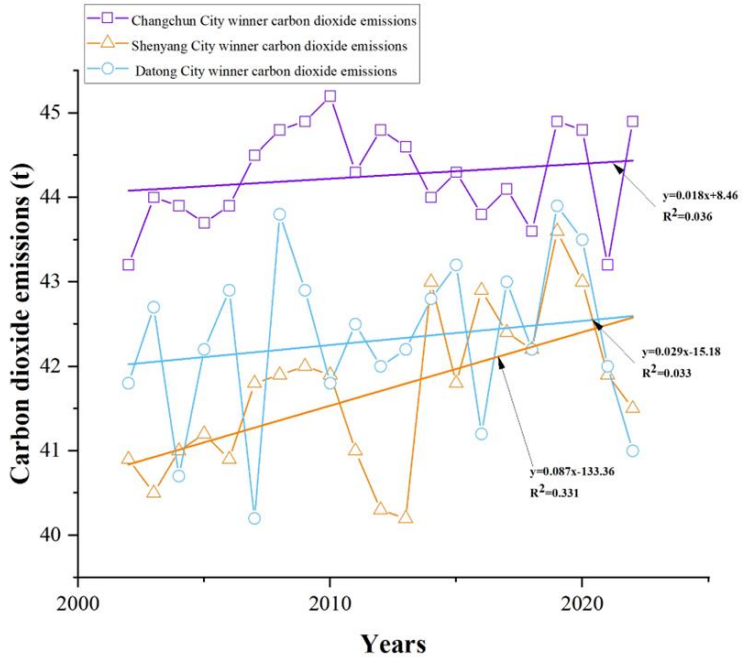

Figure 13. CO_2 emissions in the winter of Changchun City, Shenyang City, Datong City in the past 20 years

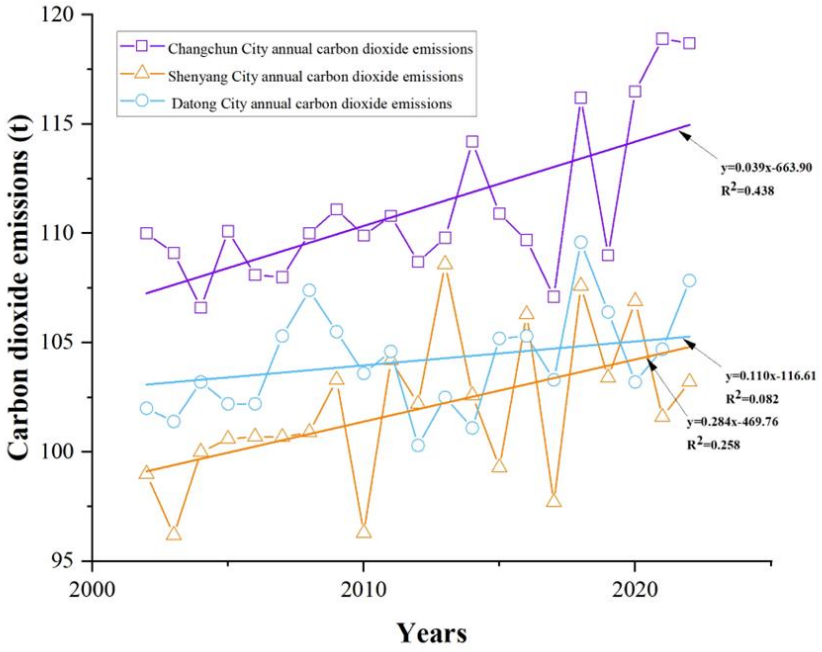

Figure 14. CO_2 emissions from this building in Changchun City, Shenyang City, Datong City in the past 20 years

4.4. Summary of this Chapter

This chapter selects the temperature changes in three severe cold regions in Changchun City of Jilin Province, Shenyang City of Liaoning Province, and Datong City of Shanxi Province in the past 20 years as calculation data. Using NASA Goddard Earth Science as the data source, we analyzed the spring, summer, autumn, winter and average temperature changes in these three cities in the past 20 years, and simulated the impact of the summer, autumn, winter and annual average temperature changes on carbon dioxide emissions in the past 20 years, clearly the graph below shows the impact of seasonal temperature changes and annual temperature changes on building carbon emissions in severe cold regions.

5.The Impact of Changes in Building Structure on Carbon Dioxide Emissions throughout the Building’s Life Cycle

Building materials will cause huge carbon dioxide emissions not only in the production stage but also in the building use stage, and different building materials have different impacts on the carbon dioxide produced in the building use stage. Since trees can gather and fix carbon dioxide during their growth process, this chapter will consider changing the building materials from reinforced concrete to wood and replacing the reinforced concrete structure with a wooden structure building using wood as new material, to calculate the life cycle carbon dioxide emissions for two structures.

5.1. Wooden structure building model parameters

The wooden structure building in this article and the original structure building has the same building structure and the same shape coefficient of 0.28. However, due to the different design standards for wooden structures and reinforced concrete building design standards, the design of timber is based on the Standard for Design of Timber Structure[63]. The wooden structure parameters are in table 2.

Table2. Wooden design parameters

Design Parameters	Data	Heat transfer coefficient
Exterior wall	403*mm* specification board+60*mm*EPS polystyrene foam board	0.24
Roof	*210mm* oriented strand board+50*mm*EPS polystyrene foam board	0.16
Exterior window	4+10(A)+4 single silver Low-e+10(Ar)+4，ordinary hollow glass plastic steel window	2.0
Floor height	2.8m	
Indoor temperature	not lower than 18℃、not higher than 26℃	
Air exchanges	0.5 times/h	
Power density of lighting	5W/m^2	
Power density of equipment	3.8W/m^2	
Personnel	two persons in the bedroom, three persons in the living room, and one person in other rooms.	
Heating method	centralized heating	
Cooling	air conditioning	
Window-to-wall ratio	North：0.20 East：0.25 South：0.30 West：0.25	

5.2. Carbon Emissions During the Material Production stage

In this paper, reinforced concrete structures and wood structures are selected for a comparative study of life cycle carbon emissions. According to GB51366-2019-T "Carbon Emission Calculation Standard for Buildings"[64] , Carbon emissions in the production stage of building materials should be calculated according to Equation 8.

$$C_{sc} = \sum_{i=1}^{n} M_i F_i \quad (8)$$

Where: C_{sc} is the carbon emission of the production stage of building materials ($kgCO_2e$); M_i is the consumption of the i major building material; F_i is the carbon emission factor of the i major building material ($kgCO_2e$/unit quantity of building materials)

Since China does not have clear relevant regulations on the carbon sequestration and carbon emission factors of wood(only the Guidelines for the Construction of Carbon Peak Carbon Neutral Standard System was published on April 1, 2023), by reading a large amount of literature , we can determine the carbon sequestration coefficient of wood growth. It can be concluded that the carbon sequestration coefficient for wood growth (f_g): f_g =889.3 kg/m^3 [65][66][67], Therefore, the carbon emissions from the production stage of wood structures are calculated according to Equation 9 and Equation 10.

$$C_z = -C_g + \sum_{i=1}^{n} m_i \times f_{pi} \quad (9)$$

$$C_g = m \times f_g \quad (10)$$

Where: C_z is the total carbon emissions from the production of building materials; C_g is the amount of carbon sequestered by wood; f_{pi} is the CO_2 emission factor; m is the mass of wood.

According to the carbon emission factors in the China Life Cycle Database (CLCD) from Chinese Carbon Footprint Open Platform(CCFOP)[64],

the CO_2 emission factors of the material production stage are shown in Table 3 and Table 4.

Table 3. Carbon emission factors of building materials.

Construction material category	Carbon emission factors for building materials
Sand	2.51 $kgCO_2e/t$
Gravel	2.18 $kgCO_2e/t$
Polystyrene foam board	5020 $kgCO_2e/t$
Ordinary silicate cement (market average)	735 $kgCO_2e/t$
Hot rolled carbon steel bars	2340 $kgCO_2e/t$
Rock wool panels	1980 $kgCO_2e/t$

Table 4. CO_2 emission factor per cubic meter of wood processed.

Material type	Material specific gravity kg/m^3	CO_2 emission factor $kgCO_2e/m^3$
Specification board	450	151.58
Oriented strand board	460	271.2

5.3. Carbon Emissions in the Production Stage of the Original Structural Building Materials

Since this paper is a cast-in-place concrete frame structure, the five main components of raw materials, cement, sand, gravel, steel, and insulation board, are selected. The amount of cement, sand, gravel, steel and insulation board in the project is calculated according to the drawings of the project. 81.05 tons of cement, 145.06 tons of sand, 74.72 tons of gravel, 37.35 tons of steel, and 2.07 tons of polystyrene. Because there is no difference in carbon dioxide emissions during the material production stage whether in Shenyang City, Changchun City, or Datong City.

According to Equation 8, C_{sc} =147.50tCO_2e.

5.4. Carbon Emissions in the Production Stage of Wood Construction Materials

According to calculations based on the engineering structure drawing, the number of materials used after the building is converted to a wooden structure is: 7.2t of cement, 2.93t of sand, 5.49t of gravel, 15.12t of steel and 0.85 tons of polystyrene. Based on literature review, Specification boards and oriented strand boards were selected. The specification boards are 72.7m^3 and the oriented strand boards are 98.5m^3. Because there is no difference in carbon dioxide emissions during the material production stage whether it is Shenyang City, Changchun City or Datong City.

According to Equation 9 and Equation 10, C_z =-69.55tCO_2e

5.5. Carbon Emissions in Material Transportation Stage

The material transportation stage refers to the transportation process including the transportation of raw materials to the place of material production and the process of transporting finished and semi-finished materials from the place of material production to the construction site. Carbon emissions in this transportation stage mainly come from transportation.

According to Standard for Building Carbon Emission Calculation[64], when the transportation distance of building materials is unknown, the

transportation distance of reinforced concrete is 40km and that of other materials is 500km.The carbon emission in the transportation stage of building materials should be calculated according to Equation 11.

$$C_{ys} = \sum_{i=1}^{n} M_i D_i T_i \quad (11)$$

Where, C_{ys} is the carbon emission of the transportation process of building materials ($kgCO_2e$); M_i is the consumption of i main building materials (t); D_i is the average transportation distance of building materials (km); T_i is the carbon emission factor per unit weight of transportation distance under the transportation mode of building materials $kgCO_2e/(t.km)$.

Table 5. Carbon emission factors of transportation modes.

Type of shipping method	Carbon emission factors
Light diesel truck transport (2t load)	0.286
Heavy-duty diesel truck transportation (30t load)	0.078
Heavy-duty diesel truck transportation (46t load)	0.057
Rail transportation (China market average)	0.010
Container ship transportation (200 TEU capacity)	0.012

5.6. Carbon Emissions in the Transportation Stage of Original Structural Building Materials

81.05 tons of cement, 145.06 tons of sand, 74.72 tons of gravel, 37.35 tons of steel, and 2.07 tons of polystyrene. According to the actual weight, and as far as possible to reduce carbon emissions decided to transport vehicles for 81.05 tons of cement for the load 30t heavy-duty diesel truck transport, 145.06 tons of sand for the load 46t heavy-duty diesel truck transport, 74.72 tons of gravel for 46t heavy-duty diesel truck transport, 37.35 tons of steel for the load 30t heavy-duty diesel truck transport, 2.07 tons of insulation board for the load 2t light diesel truck. The transportation distance of reinforced concrete is 40km and that of other materials is 500km[64]. Since it is a simulation calculation, the transportation distances of Changchun, Shenyang and Datong are all set to the transportation distance of reinforced concrete is 40km and that of other materials is 500km[64]. There is no difference in carbon dioxide emissions in the material transportation stage between the three cities.

According to Equation 11, C_{ys} =4.71tCO_2e.

5.7. Carbon Emissions in the Transportation Stage of Wood-frame Buildings

The Specification board is 113.5m^3 and the oriented strand board is 240.79m^3. They all choose to be transported locally. The transportation distance of reinforced concrete is 40km and that of other materials is 500km[64]. A 30-ton heavy-duty diesel truck will be selected as a tool for transportation from the timber market to the construction site. Cement, sand, gravel, and steel are all transported locally. 2-ton light diesel truck transports 7.2 tons of cement, a 2-ton light diesel truck transports 2.93 tons of sand, a 2-ton light diesel truck transports 5.49 tons of gravel, a 2-ton light diesel truck transports 15.12 tons of steel, and a 78.03 ton wood board uses a 2-ton light Diesel truck transportation, the transportation distance of reinforced concrete is 40km and that of other materials is 500km[64]. There is no difference in carbon dioxide emissions in the material transportation stage between the three cities.

According to Equation 11, C_{ys} =6.74tCO_2e.

5.8. Construction Stage of the Carbon Emissions

The carbon emission in the construction stage of building shall include the carbon emission generated by the completion of each sub-project construction and the carbon emission generated by the implementation process of each measure project.

For the construction project, the scope of construction has been relatively clear, consider the construction sub-projects, the bill of quantities to divide the building construction into the main parts such as earthwork, foundation and foundation works, main structure of the building, scaffolding works, form works, etc. On this basis, define it as the carbon emission of the main construction process, then refine each process again, and finally the carbon emission of each engineering process is divided according to Finally, the carbon emission of each engineering process is added up according to the division, and the total carbon emission of the whole construction activity is obtained. According to GB51366-2019-T "Carbon Emission Calculation Standard for Construction"[64], the carbon emission in the construction stage of building should be calculated according to Equation 12.

$$C_{jz} = \sum_{i=1}^{n} E_{jz,i} EF_i \quad (12)$$

Where: C_{jz} is the carbon emission of the building construction stage (tCO_2e); $E_{jz,i}$ is the total energy use of the building construction stage *(kWh/kg)*, EFi is the carbon emission factor of the energy type ($kgCO_2/kWh$ or $kgCO_2/kg$).

The carbon emission factors according to the China Life Cycle Database (CLCD) from Chinese Carbon Footprint Open Platform(CCFOP)[64], are shown in Table 6 and Table 7.

Table 6. Fossil fuel carbon emission factors.

Fuel Type	CO_2 emission factor per unit calorific value *(tCO_2/TJ)*
Gasoline	67.91
Diesel	72.59

Table 7. Average CO_2 Emission Factor of China's Regional Power Grids in 2012

Grid name	Emission factor *($kgCO_2/kWh$)*
Northeast Regional Grid	0.7769

5.9. Carbon Emission of the Original Structure Building Construction Process

The amount of work and consumption of gasoline, diesel fuel and electrical consumption of the machinery during the construction stage of the building were calculated from the architectural drawings. The quantities of works and consumption during the construction of the prototype structure are summarized in Table 8.

There is no difference in carbon dioxide emissions during the construction stage between Changchun City, Shenyang City and Datong City.

According to Equation 12, C_{jz} =34.06tCO_2e.

Table 8. Summary of construction process works and consumption of the original structure building

Construction stage machinery	Quantity of work	Gasoline consumption (*kg*)	Diesel consumption (*kg*)	Electrical consumption (*kWh*)
Crawler bulldozer function	2.64		347.03	
Crawler type single bucket excavator	1.38		102.00	
Dump truck	111.09	5370.45		
Electric tamper	100.77			4172.67
Static pile driver	6.59		679.44	
Truck-mounted cranes	9.47		469.23	
Crawler type diesel pile driver	23.00		1328.79	
AC arc welding machine	7.53			601.77
Mortar mixer	5.11			44.00
Concrete mixer	9.35			514.62
Concrete transfer pumps	13.91			3986.53
Electric winch	66.57			2514.53
Prestressing Steel Tensioning Machine	0.49			8.45
Rebar cutting machine	3.94			126.47
Rebar bending machine	9.76			124.93
Spot welding machine	11.52			1781.34
Butt welding machine	2.04			248.88
Flat water grinding machine	56.26			787.5
Truck-mounted cranes	1.24	392.69		
Truck	7.02		228.87	
Total		5763.14	3155.36	14911.69

5.10. Carbon Emissions During the Construction of Wood-frame Buildings

The amount of work during the construction stage of the building and the electricity consumption of gasoline, diesel fuel and machinery were calculated based on the architectural drawings. The summary table of the amount of work and consumption during the construction of the wood structure is shown in Table 9.

According to Equation 12, C_{jz} =27.09tCO_2e.

Table 9. Summary of construction process works and consumption of wood-frame building

Construction stage machinery	Quantity of work	Gasoline consumption (*kg*)	Diesel consumption (*kg*)	Electrical consumption (*kWh*)
Crawler bulldozer function	2.64		449.04	
Crawler type single bucket excavator	1.38		93.00	
Dump truck	111.09	4300.45		
Electric tamper	100.77			4172.67
Concrete mixer	0.83			
Electric winch	10.19			
Prestressing Steel Tensioning Machine	0.16			
Rebar cutting machine	1.16			601.77
Rebar bending machine	3.25			44.00
AC arc welding machine	1.36			514.62
Spot welding machine	3.84			3986.53
Electric winch	0.68			2514.53
Butt welding machine	15.21			8.45
Woodworking circular sawing machine	10.01			126.47
Woodworking Eyelet Punching Machine	17.14			124.93
Woodworking flat blasting machine	2.34			1781.34
Mortar mixer	2.04			248.88
Flat water grinding machine	56.26			787.5
Truck	0.21	518.14	6.78	
Fork lift	16.17			
Total		4818.59	548.82	14911.69

5.11. Carbon Emissions in Operation Stage

The operational stage carbon emissions are the carbon emissions generated from the overall operation of the building over its 50-year lifecycle. The carbon footprint of the building is obtained by simulating the thermal performance, lighting system, and human activities to the same values and using DesignBuilder softward.

5.12. Carbon Emissions in the Operational Stage of Original Structure Buildings

Through DesignBuilder software simulation, it can be concluded that the annual carbon dioxide emissions of this building in Changchun City in 2022 are 118.7 tCO_2, the annual carbon dioxide emissions of this building in Shenyang City in 2022 are 107.84tCO_2, and the annual carbon dioxide emissions of this building in Datong City in 2022, The carbon emission is 103.21tCO_2. so the total carbon emission during the operation stage of the original structure building ：

Changchun City: C_{yy} =5935tCO_2e,

Shenyang City: C_{yy} =5392tCO_2e.

Datong City: C_{yy} =5160.5tCO_2e,

Among them, the carbon dioxide emissions from the heating are 4854tCO_2 in Changchun, 4611tCO_2 in Shenyang, and 4527tCO_2 in Datong. The carbon dioxide emissions from the cooling are 171tCO_2 in Changchun, 161tCO_2 in Shenyang, and 154tCO_2 in Datong.

5.13. Carbon Emissions in the Operational Stage of Wood-frame Buildings

Through DesignBuilder software simulation, it can be concluded that the annual carbon dioxide emissions of this building in Changchun City in 2022 are 85.13tCO_2, the annual carbon dioxide emissions of this building in Shenyang City in 2022 are 80.10tCO_2, and the annual carbon dioxide emissions of this building in Datong City in 2022 The carbon emission is 75.24tCO_2. so the total carbon emission during the operation stage of the prototype structure building：

Changchun City: C_{yy} =4265tCO_2e,

Shenyang City: C_{yy} =4022tCO_2e.

Datong City: C_{yy} =3754tCO_2e,

Among them, the carbon dioxide emissions from the heating are 3531.5tCO_2 in Changchun, 3342.5tCO_2 in Shenyang, and 3907.5tCO_2 in Datong. The carbon dioxide emissions from the cooling are 163tCO_2 in Changchun City, 152.5tCO_2 in Shenyang City, and 147.5tCO_2 in Datong City.

The carbon dioxide emissions during the cooling and heating of the building operational stage are shown in Figure 15.

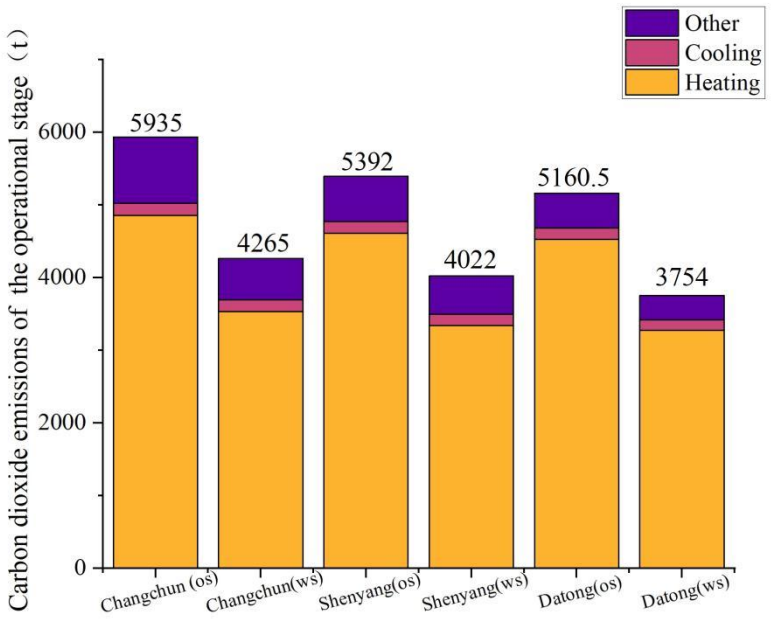

Figure 15. The carbon dioxide emissions chart of the operational stage in Changchun City, Shenyang City, and Datong City

5.14. Carbon Emissions in the Demolition Stage

The carbon emission of building demolition processing stage refers to the carbon emission generated by the construction of the building in the demolition stage, which can be calculated according to the volume of demolition construction stage, according to GB51366-2019-T "Carbon Emission Calculation Standard for Construction"[64], the carbon emission of building materials demolition stage should be calculated according to Equation 13.

$$C_{cc} = \sum_{i=1}^{n} E_{cc,i} EF_i \qquad (13)$$

Where: C_{cc} is the carbon emission in the demolition stage ($kgCO_2e$); $E_{cc,i}$ is the total use of the first type of energy in the building demolition stage (kWh/kg); EF_i the carbon emission factor of the type of energy ($kgCO_2e/kWh$ or $kgCO_2e/kg$).

Due to the lack of data on carbon emissions during the demolition stage in China, according to estimates conducted by relevant scholars, the building demolition stage usually accounts for 90% of the energy consumption during the construction stage of building construction[64].

5.15. Carbon Emissions During the Demolition Stage of Original Structure Building

Taking the carbon emissions during the demolition stage as 90% of its construction stage, the carbon emissions during the demolition stage of the reinforced concrete structure are 30.65tCO_2.

5.16. Carbon Emissions in the Demolition Stage of Wood-frame Buildings

Taking the carbon emissions during the demolition stage of a wooden frame building as 90% of the construction stage, the carbon emissions during the demolition stage of a wooden frame building are 24.38tCO_2.

5.17. Comparison of Life-cycle Carbon Dioxide Emissions between the Original Structure Buildings and the Wooden Structures

Since there is no clear regulation on the recycling of construction waste stage in China, the CO_2 emission in the recycling of construction waste stage is not calculated in the life cycle carbon emission calculation.

The life cycle carbon emissions (OS):

Changchun City: $C = C_{sc} + C_{ys} + C_{jz} + C_{yy} + C_{cc}$ =6151.92tCO_2e.

Shenyang City: $C = C_{sc} + C_{ys} + C_{jz} + C_{yy} + C_{cc}$ =5608.92tCO_2e.

Datong City: $C = C_{sc} + C_{ys} + C_{jz} + C_{yy} + C_{cc}$ =5377.42tCO_2e.

The life cycle carbon emission of wooden structures (WS):

Changchun City: $C = C_{sc} + C_{ys} + C_{jz} + C_{yy} + C_{cc}$ =4253.66tCO_2e.

Shenyang City: $C = C_{sc} + C_{ys} + C_{jz} + C_{yy} + C_{cc}$ =4010.66tCO_2e.

Datong City: $C = C_{sc} + C_{ys} + C_{jz} + C_{yy} + C_{cc}$ =3742.66tCO_2e.

According to Figure 16, it can be concluded that compared with the life cycle carbon emissions of the original structure buildings in Changchun City, the life cycle carbon emissions of the wooden structure buildings were reduced by 1898.26 tCO_2e, and the life cycle carbon emissions of the wooden structure buildings were reduced by 30.8%. The carbon dioxide emissions of wooden structure heating are 1322.5t less than the carbon dioxide emissions of original structure heating, and the reduction rate is 22.28% compared with the total carbon dioxide emissions from the original structure building. The carbon dioxide emissions of wooden structure cooling are 8t less than the carbon dioxide emissions of original structure cooling, and the reduction rate is 0.13% compared with the total carbon dioxide emissions from the original structure building.

Compared with the life cycle carbon emissions of the original structural buildings in Shenyang City, the life cycle carbon emissions of wooden structure buildings have been reduced by 1598.26 tCO_2e, and the life cycle carbon emissions of wooden structure buildings have been reduced by 28.5%.The carbon dioxide emissions of wooden structure heating are 1268.5t less than the carbon dioxide emissions of original structure heating, and the reduction rate is 23.52% compared with the total carbon dioxide emissions form the original structure building. The carbon dioxide emissions of wooden structure cooling are 8.5t less than the carbon dioxide emissions of original structure cooling, and the reduction rate is 0.16% compared with the total carbon dioxide emissions from the original structure building.

Compared with the life cycle carbon emissions of the original structural buildings in Datong City, the life cycle carbon emissions of wooden structure buildings have been reduced by 1634.76 tCO_2e, and the life cycle carbon

emissions of wooden structure buildings have been reduced by 30.5%.The carbon dioxide emissions of wooden structure heating are 1253t less than the carbon dioxide emissions of original structure heating, and the reduction rate is 24.28% compared with the total carbon dioxide emissions from the original structure building. The carbon dioxide emissions of wooden structure cooling are 6.5t less than the carbon dioxide emissions of original structure cooling, and the reduction rate is 0.12% compared with the total carbon dioxide emissions form the original structure building.

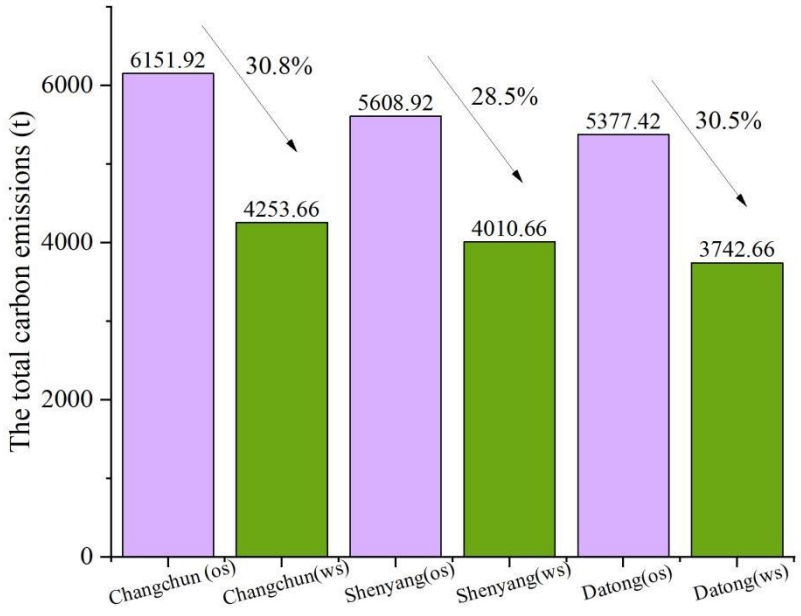

Figure 16. Life cycle carbon dioxide emissions chart of original structure buildings and wooden structure buildings in Changchun City, Shenyang City, and Datong City

5.18. Summary of this Chapter

This chapter selects the original building structure - reinforced concrete structure and the new building structure - wooden structure uses the inventory analysis method to analyze the construction stage and compare the carbon dioxide emissions of the material production stage, the transportation stage, the construction stage, the operation stage, the demolition stage throughout the building life cycle. and the wooden structure significantly reduces carbon dioxide emissions compared to the reinforced concrete structure.

6. Building Carbon Dioxide Emissions Caused by Changes in Building Envelope

The thermal performance of the building envelope is a key factor affecting the carbon emissions and energy consumption of residential buildings in severe cold regions. The heat loss through the building envelope accounts for 70% to 80% of the heat loss of the building[68][69][70]. According to calculations, the heat transfer coefficients of exterior walls, exterior windows, roofs and other enclosure structures of residential buildings in severe cold regions in China are 3-5 times that of developed countries at the same latitude. Therefore, this chapter selects exterior windows, exterior walls, and roofs as design parameters and uses Design Builder software to simulate carbon emissions.

6.1. Modification Parameters

Since Changchun City, Shenyang City, and Datong City all belong to severe cold regions (C) stipulated in the "Residential Building Design Standards (Energy Saving 75%)"[71], they have the same design parameter requirements for building envelopes. Therefore, this type of exterior windows and exterior walls, the same parameters are selected for roof design optimization.

According to the "General Specifications for Building Energy Conservation and Renewable Energy Utilization "[72], the thickness of the exterior wall of the building shall not exceed 490*mm*. Therefore, the thickness of the exterior wall EPS polystyrene foam board insulation layer is selected from 60-80*mm*, and one data is selected every 5*mm*. A total of 5 data are used as variables for simulation. The thickness of the roof EPS polystyrene foam board is selected from 50*mm*-100*mm*, and one data is selected every 5*mm*. A total of 10 data are used as variables for simulation. Based on the general atlas "Energy-Saving Doors and Windows"[73], A total of 5 data are used as variables for simulation. Therefore, the design plan for the transformation parameters is shown in Table 10-12.

Table 10. Modification parameter design plan (MP)-External wall insulation thickness

External wall insulation thickness(mm)	Heat transfer coefficient ($W/(m^2 \cdot K)$)
MP1=65	0.391
MP2=70	0.387
MP3=75	0.368
MP4=80	0.342
MP5=85	0.323

Table11. Modification parameter design plan (MP)—Roof insulation thickness.

Roof insulation thickness (mm)	Thermal transmittance ($W/(m^2 \cdot K)$)	Roof insulation thickness (mm)	Thermal transmittance ($W/(m^2 \cdot K)$)
MP6 = 55	0.191	MP11 = 80	0.151
MP7 = 60	0.183	MP12 = 85	0.145
MP8 = 65	0.175	MP13 = 90	0.139
MP9 = 70	0.168	MP14 = 95	0.130
MP10 = 75	0.159	MP15 = 100	0.112

Table 12. Modification parameter design plan (MP)—Exterior window.

Exterior window	Thermal transmittance $(W/(m^2 \cdot K))$	Solar heat gain coefficient (SHGC)
MP16 = Plastic steel frame and triple glass window 5 + 9 (A)+ singe silver 4Low-e + 12 (Ar) + 5	1.47	0.503
MP17 = Plastic steel frame and triple glass window 3 + 11 (A) + double silver 3Low-e + 11 (Ar) + 3	1.40	0.518
MP18 = Plastic steel frame and triple glass window 4 + 10 (A) + double silver 4Low-e + 10 (Ar) + 4	1.34	0.511
MP19 = Plastic steel frame and double glass window 6 + Vacuum + 6 singe silver Low-e	1.13	0.562
MP20 = Plastic steel frame and triple glass window 6 + Vacuum + 6 double silver Low-e + PolyVinyl Butyral Film + 6	0.95	0.541

6.2. Parameter Change Comparison and Simulation

The original design plan model was modified 20 times in accordance with the project's current circumstances. To determine the carbon dioxide reduction rate of the design retrofit programs based on the simulation findings, apply the computational model of carbon dioxide reduction rate Equation (1).

6.2.1. Exterior Wall

Use Designbuilder software to simulate carbon dioxide emissions in Changchun City and Shenyang Datong City respectively. Based on the original design of annual carbon dioxide emissions, the relationship between MP1-MP5 and the emission reduction rate is shown in Figure 17.

As can be seen from Figure 17, in Changchun, Shenyang and Datong cities, in terms of exterior wall design, increasing the thickness of insulation materials is positively correlated with reducing the carbon dioxide emissions of buildings, and as the thickness of insulation materials increases, carbon dioxide emissions gradually decrease. In Changchun City, when the thickness of EPS polystyrene foam board is 85*mm*, the carbon emission reduction rate can reach a maximum of 3.53. In Shenyang City, when the thickness of EPS polystyrene foam board is 85*mm*, the carbon emission reduction rate can reach a maximum of 3.42. In Datong City, when the thickness of EPS polystyrene foam board is 85*mm*, the maximum carbon emission reduction rate can reach 3.34. This shows that increasing the thickness of exterior wall insulation of residential buildings in severe cold regions is effective in reducing carbon dioxide emissions.

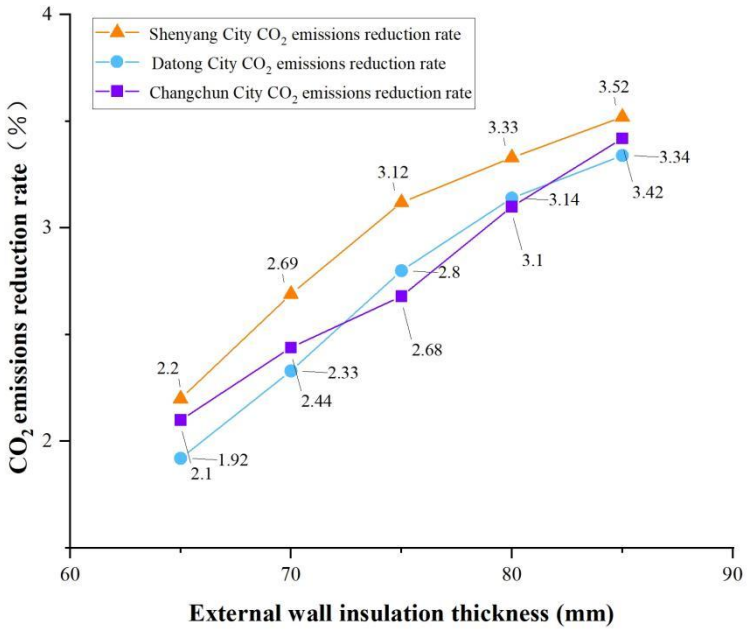

Figure 17. CO_2 emission reduction rate of different external walls insulation thickness in Changchun City、Shenyang City、Datong City .

6.2.2. Roof

Based on the original designed annual carbon dioxide emissions, the relationship between MP6 and MP15 and the emission reduction rate is shown in Figure 18.

As can be seen from Figure 18, in terms of roof design in Changchun City, Shenyang City and Datong City, increasing the thickness of insulation materials is positively correlated with reducing the carbon dioxide emissions of buildings, and as the thickness of insulation materials increases, carbon dioxide emissions gradually decrease. In Changchun City, when the thickness of EPS polystyrene foam board is 100*mm*, the emission reduction rate can reach a maximum of 5.3. In Shenyang City, when the thickness of EPS polystyrene foam board is 85*mm*, the maximum emission reduction rate can reach 3.9. In Datong City, when the thickness of EPS polystyrene foam board is 85*mm*, the maximum emission reduction rate can reach 4.89. This shows that increasing the thickness of roof insulation of residential buildings in severe cold regions is effective in reducing carbon dioxide emissions. But the benefit diminishes as the insulation layer thickness increases.

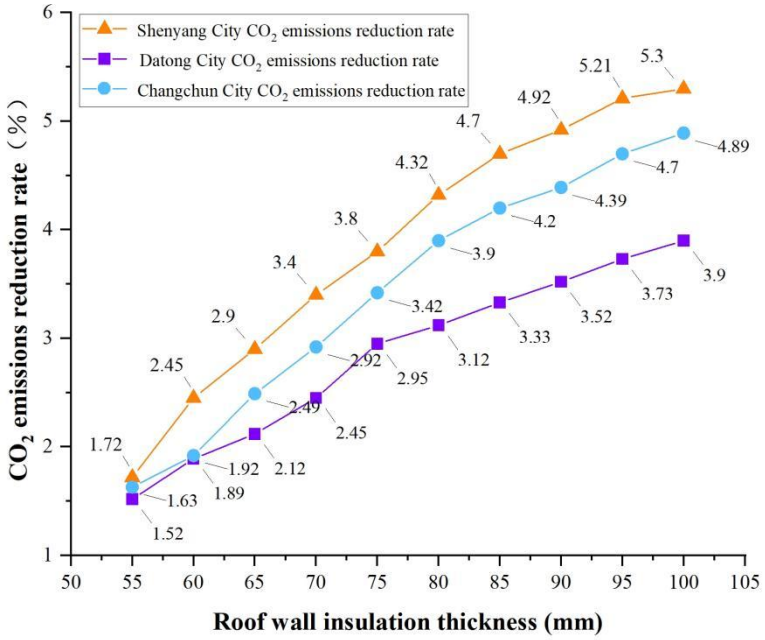

Figure 18. CO_2 emission reduction rate of different roof insulation thickness in Changchun City, Shenyang City, Datong City .

6.2.3. External Windows

Based on the original designed annual carbon dioxide emissions, the relationship between MP16 and MP20 and the emission reduction rate is shown in Figure 19.

As can be seen from Figure 19, in Changchun City, the MP20 project has the highest carbon dioxide emission reduction rate, reaching 7.2%. In Shenyang City, the MP20 project has the highest carbon dioxide emission reduction rate, reaching 6.3%. In Datong City, the MP20 project has the highest carbon dioxide emission reduction rate, reaching 6%. This suggests that installing high-performance exterior windows in residential buildings in severe cold regions can help reduce CO_2 emissions. Therefore, in severe cold regions, windows with large SHGC values should be selected. According to the "Optical and Thermal Performance of Glass Curtain Wall"[74] , the SHGC should not be greater than 0.75 in severe cold regions. Therefore, when the *K* values are similar or the same, windows with larger SHGC values should be selected as much as possible to reduce heat loss and thereby reduce carbon dioxide emissions.

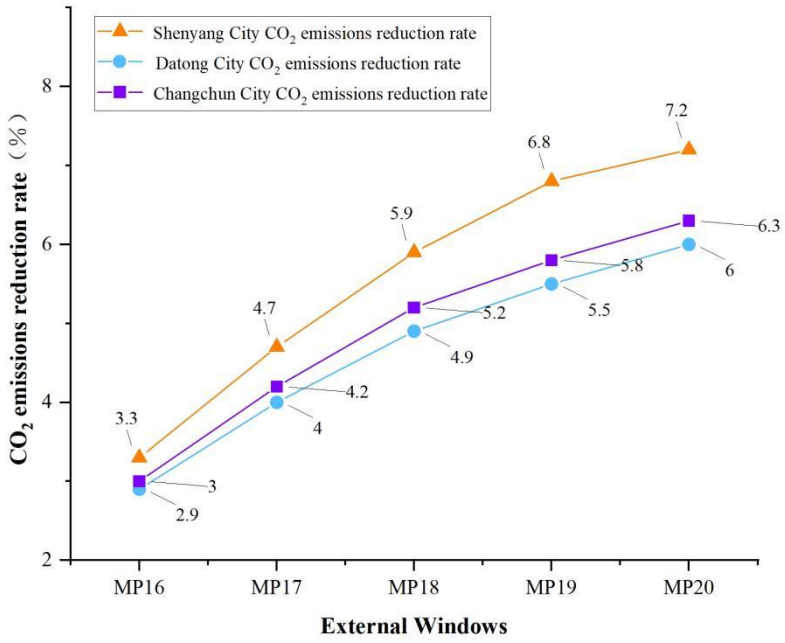

Figure19. CO_2 emission reduction rate of different window types in Changchun City, Shenyang City, Datong City .

6.3. Optimal Parameter Design Plan

Factors affecting residents carbon emissions need to be considered to obtain the best parameter transformation plan. This chapter selects three factors that affect the annual carbon emissions of residential buildings: exterior wall A, roof B and exterior window C. Each influencing factor is divided into four levels. The orthogonal method is used to test and obtain the optimal parameter design plan. From the above simulation results, we can see that the thickness of the exterior wall insulation layer, the heat transfer coefficient of the exterior windows, and the thickness of the roof insulation layer are positively correlated with annual carbon emissions. The influencing factors and levels of the orthogonal method are shown in Table13.

Table 13. Table of orthogonal levels and factors.

Level	Exterior Wall A	Roof B	External Window C
1	70 *mm* EPS polystyrene foam board(A1)	80 *mm* EPS polystyrene foam board(B1)	Plastic steel frame and triple glass window 3 + 11(A) + 3 double silver Low-e + 11 (Ar) + 3 (C1)
2	75 *mm* EPS polystyrene foam board (A2)	90 *mm* EPS polystyrene foam board(B2)	Plastic steel frame and triple glass window 4 + 10 (A) + 4 double silver Low-e + 10 (Ar) + 4(C2)
3	80 *mm* EPS polystyrene foam board(A3)	95 *mm* EPS polystyrene foam board(B3)	Plastic steel frame and double glass window 6 + Vacuum + 6 singe silver Low-e(C3)
4	85 *mm* EPS polystyrene foam board(A4)	100 *mm* EPS polystyrene foam board(B4)	Plastic steel frame and triple glass window 6 + Vacuum + 6 double silver Low-e + PolyVinyl Butyral Film + 6 (C4)

6.3.1. Visual Analysis

As this paper selects three influences and four levels, the $L_{16}(3^4)$ orthogonal table was chosen. Since this article selects three cities in severe cold regions of Changchun City, Shenyang City, and Datong City as simulation objects, this article will establish three orthogonal analysis tables. As shown in Table14-16.

In Table 14-16, K_1, K_2, K_3, and K_4, respectively, represent the total annual carbon emissions of the building under the various factors and levels, and $\overline{K_1}$, $\overline{K_2}$, $\overline{K_3}$, and $\overline{K_4}$ represents the average annual carbon emissions of the building under the various factors and levels. Since the number of levels may be different, the average annual carbon emissions and annual energy consumption are generally used to reflect the degree of influence of different levels of the same factor on the test results and to determine the best value for this factor level. The range value *R* of the average value at each level of the same factor is used to reflect the influence of the level changes in each factor on the test results. The greater the *R*-value, the greater the impact of the factor level change on the test results, and vice versa.

It can be seen from Figure 20 that for Changchun City, the main influencing factors of project annual carbon emissions are exterior walls (A), exterior windows (C) and roofs (B). The best solution to reduce carbon emissions in Changchun City is A4B4C4, 85*mm* EPS polystyrene foam board (A4), 100*mm* EPS polystyrene foam board (B4), plastic steel frame and triple-glazed windows 6+Vacuum+6 double silver Low-e+PolyVinyl Butyral Film+6(C4)). However, the optimal parameter design plan is not in the 16 test combinations and requires validation experiments.

It can be seen from Figure 21 that for Shenyang City, the main influencing factors of project annual carbon emissions are exterior walls (A), roofs (B), and exterior windows (C). The best solution to reduce carbon emissions in Shenyang City is A4B4C4, 85*mm* EPS polystyrene foam board (A4), 100*mm* EPS polystyrene foam board (B4), plastic steel frame and triple-glazed windows 6+Vacuum+6 double silver Low-e+PolyVinyl Butyral Film+6(C4)). However, the optimal parameter design plan is not in the 16 test combinations and requires validation experiments.

It can be seen from Figure 22 that for Datong City, the main influencing factors of project annual carbon emissions are exterior walls (A), roofs (B), and exterior windows (C). The best solution to reduce carbon emissions in Datong

City is A4B4C4, 85*mm* EPS polystyrene foam board (A4), 100*mm* EPS polystyrene foam board (B4), plastic steel frame and triple-glazed windows 6+Vacuum+6 double silver Low-e+PolyVinyl Butyral Film+6(C4)). However, the optimal parameter design plan is not in the 16 test combinations and requires validation experiments.

Table 14. Orthogonal test table in Changchun City.

	Test Count	Exterior Wall A	Roof B	External Window C	Carbon Emissions *(t)*
	1	A1	B1	C1	100.32
	2	A1	B2	C2	99.71
	3	A1	B3	C3	98.79
	4	A1	B4	C4	97.74
	5	A2	B1	C2	99.08
	6	A2	B2	C1	98.56
	7	A2	B3	C4	96.92
	8	A2	B4	C3	97.22
	9	A3	B1	C3	97.52
	10	A3	B2	C4	96.84
	11	A3	B3	C1	97.02
	12	A3	B4	C2	96.60
	13	A4	B1	C4	95.82
	14	A4	B2	C3	95.93
	15	A4	B3	C2	95.95
	16	A4	B4	C1	95.62
Result	K1	396.56	392.74	391.52	
	K2	391.78	391.04	391.34	
	K3	387.98	388.68	389.46	
	K4	383.32	387.18	387.32	
	$\overline{K_1}$	99.14	98.19	97.88	
	$\overline{K_2}$	97.95	97.76	97.83	
	$\overline{K_3}$	97.00	97.17	97.36	
	$\overline{K_4}$	95.83	96.70	96.83	
	R1	13.24	5.56	10.2	

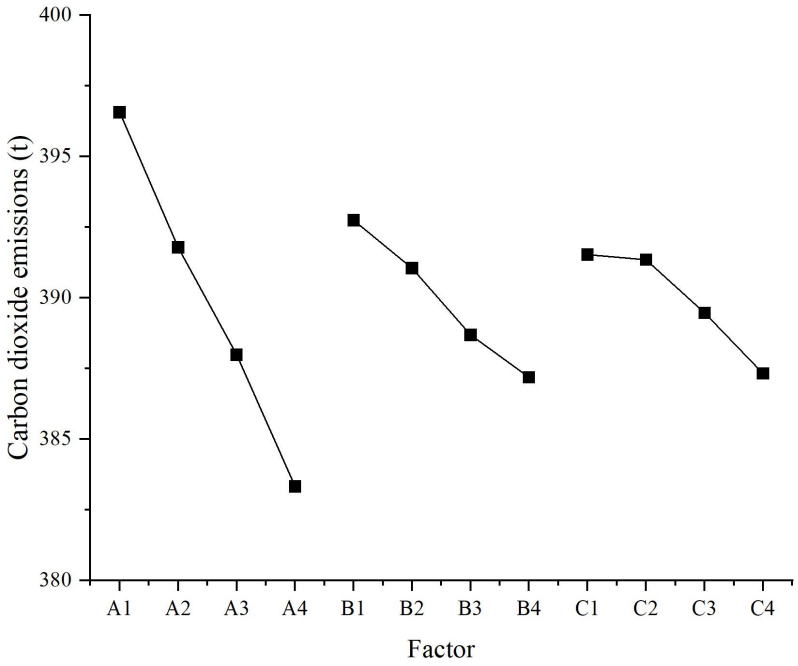

Figure 20. Factor influence trend chart in Changchun City.

Table 15. Orthogonal test table in Shenyang City.

	Test Count	Exterior Wall A	Roof B	External Window C	Carbon Emissions *(t)*
	1	A1	B1	C1	97.65
	2	A1	B2	C2	96.62
	3	A1	B3	C3	95.34
	4	A1	B4	C4	94.14
	5	A2	B1	C2	96.28
	6	A2	B2	C1	95.59
	7	A2	B3	C4	93.08
	8	A2	B4	C3	93.82
	9	A3	B1	C3	94.45
	10	A3	B2	C4	93.74
	11	A3	B3	C1	94.02
	12	A3	B4	C2	93.53
	13	A4	B1	C4	92.62
	14	A4	B2	C3	92.83
	15	A4	B3	C2	92.85
	16	A4	B4	C1	92.64
Result	K1	383.75	381	379.9	
	K2	378.77	378.78	379.28	
	K3	375.74	375.27	376.46	
	K4	370.94	374.13	373.58	
	$\overline{K_1}$	95.94	95.25	94.98	
	$\overline{K_2}$	94.69	94.70	94.82	
	$\overline{K_3}$	93.94	93.82	94.12	
	$\overline{K_4}$	92.74	93.53	93.40	
	R1	12.81	6.87	6.32	

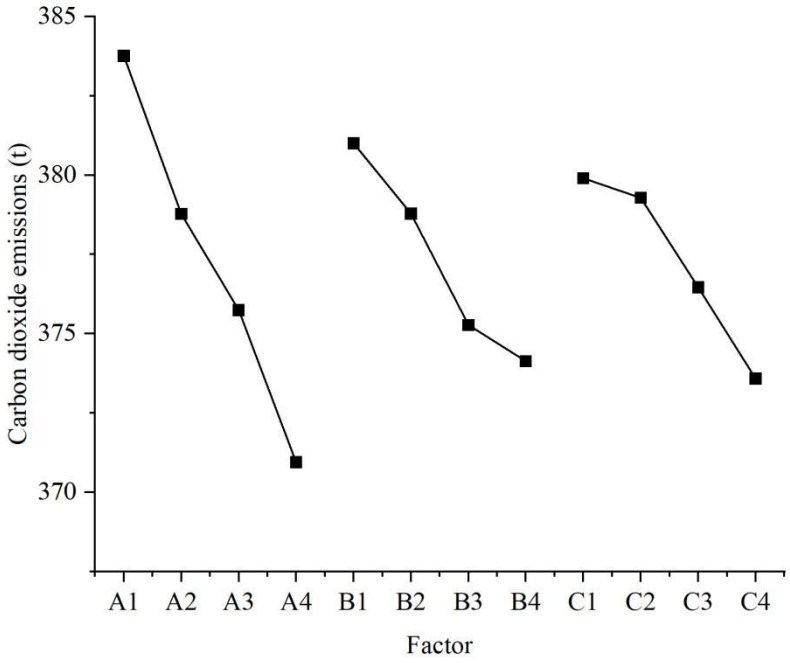

Figure 21. Factor influence trend chart in Shenyang City.

Table 16. Orthogonal test table in Datong City.

	Test Count	Exterior Wall A	Roof B	External Window C	Carbon Emissions *(t)*
	1	A1	B1	C1	98.59
	2	A1	B2	C2	97.34
	3	A1	B3	C3	96.43
	4	A1	B4	C4	95.44
	5	A2	B1	C2	97.88
	6	A2	B2	C1	96.56
	7	A2	B3	C4	94.67
	8	A2	B4	C3	95.92
	9	A3	B1	C3	95.75
	10	A3	B2	C4	94.44
	11	A3	B3	C1	95.42
	12	A3	B4	C2	94.63
	13	A4	B1	C4	93.53
	14	A4	B2	C3	93.53
	15	A4	B3	C2	93.58
	16	A4	B4	C1	93.44
Result	K1	387.8	385.75	384.01	
	K2	385.03	381.87	383.43	
	K3	380.24	380.1	381.63	
	K4	374.08	379.43	378.08	
	$\overline{K_1}$	96.95	96.44	96.00	
	$\overline{K_2}$	96.26	95.47	95.86	
	$\overline{K_3}$	95.06	95.03	95.41	
	$\overline{K_4}$	93.52	94.86	94.52	
	R1	13.72	6.32	5.93	

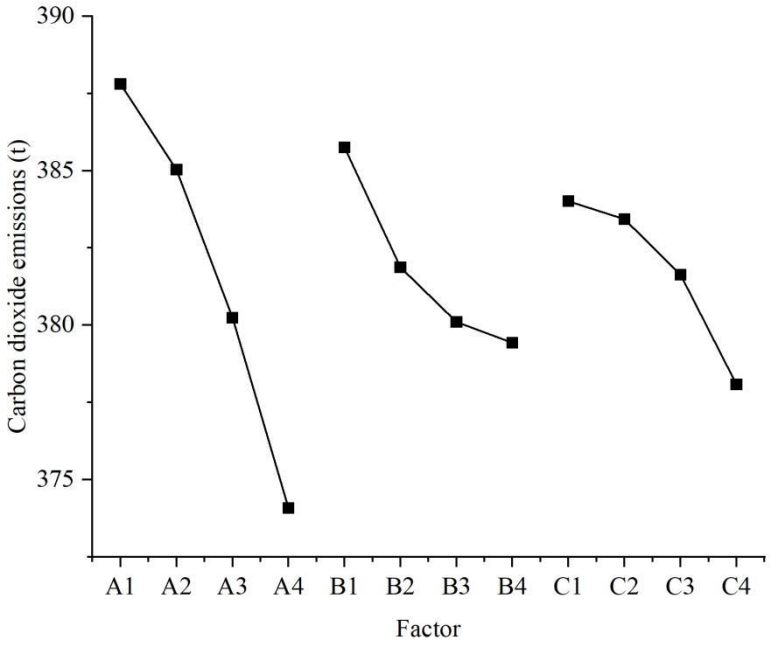

Figure22. Factor influence trend chart in Datong City.

6.4. Verification Experiment

Because the best optimal obtained is not within the range of 16 groups, verification experiments are needed for the best optimal. The best optimal in Changchun City is A4B4C4, which is 85*mm* EPS polystyrene foam board (A4), 100*mm* EPS polystyrene foam board (B4), plastic steel frame and triple-glazed windows 6+Vacuum+6 double silver Low-e+PolyVinyl Butyral Film+6(C4)). Using the best optimal in the table, test 16: A4B4C1 is 85 *mm* EPS polystyrene foam board (A4), 100 *mm* EPS polystyrene foam board (B4), Plastic steel frame and triple glass window 3+11(A)+3 single silver Low-e+11(Ar)+3(C1) conduct comparative experiments. The purpose is to verify whether the optimal solution is optimal.

Use Design Builder software to simulate two sets of experiments. It can be concluded that the annual carbon emissions of A4B4C1 are 95.62 t, and the carbon dioxide emission reduction rate is 19.44%. The annual carbon emissions of A4B4C1 are 93.47t, and the carbon dioxide emission reduction rate is 21.26%. Plan A4B4C4 is determined to be the optimal parameter design plan for residential buildings in Changchun City.

The best test combination in Shenyang City is A4B4C4, which is 85*mm* EPS polystyrene foam board (A4), 100*mm* EPS polystyrene foam board (B4), plastic steel frame and triple-glazed windows 6+Vacuum+6 double silver Low-e+PolyVinyl Butyral Film+6(C4)). Using the best combination in the table, test 16: A4B4C1 is 85 *mm* EPS polystyrene foam board (A4), 100 *mm* EPS polystyrene foam board (B4), Plastic steel frame and triple glass window 3 +11+3 single silver Low-e+11(Ar)+ 3 (C1) conduct comparative experiments. The purpose is to verify whether the solution is optimal.

Use Design Builder software to simulate two sets of experiments. It can be concluded that the annual carbon emissions of A4B4C1 are 92.64 t, and the carbon dioxide emission reduction rate is 10.24%. The annual carbon emissions of A4B4C4 are 90.47t, and the carbon dioxide emission reduction rate is 12.34%. Plan A4B4C4 is determined to be the optimal parameter design plan for residential buildings in Shenyang City.

The best test combination of Datong City is A4B4C4, which is 85*mm* EPS polystyrene foam board (A4), 100*mm* EPS polystyrene foam board (B4), plastic steel frame and triple-glazed windows 6+Vacuum+6 Double silver Low-e+PolyVinyl Butyral Film+6(C4)). Using the best combination in the table, test

16: A4B4C1 is 85 *mm* EPS polystyrene foam board (A4), 100 *mm* EPS polystyrene foam board (B4), Plastic steel frame and triple glass window 3+11(A)+3 single silver Low-e+11(Ar)+3(C1) conduct comparative experiments. The purpose is to verify whether the optimal solution is optimal.

Use Design Builder software to simulate two sets of experiments. It can be concluded that the annual carbon emissions of A4B4C1 are 93.44t, and the carbon dioxide emission reduction rate is 13.35%. The annual carbon emissions of A4B4C are 91.68t, and the carbon dioxide emission reduction rate is 14.99%. Plan A4B4C4 is determined to be the optimal parameter design plan for residential buildings in Datong City.

6.5. Economic Analysis

This article chooses the net present value as the indicator to judge whether the plan can be implemented. When the net present value is greater than 0, the plan is feasible; when net present value is less than zero, the plan is unfeasible[54].

In order to calculate the net present value data, economic calculations and analyzes were performed on the selected three parametric factors and calculation models (3) to (6) were used to determine the net present value of 16 groups of orthogonal test plans and the net present value of best design based on emission reduction options in Changchun City, Shenyang City, Datong City. Resulting in a total of 17 groups of plans, in which the standard coal market price is 0.01 *USD*/*kg*. The calorific value of standard coal is 29307.6 *kJ*/*kg*, and the combustion rate of heating coal is 0.7[75]. On July 16, 2021, the national carbon emissions trading market went online. The trading volume of the carbon emission allowance (CEA) listing agreement in the national carbon market was 4,103,953 tons, the transaction volume was *USD* 330,321,798.32, and the closing price was *USD* 8.05/ton[76]. The carbon trading price is based on the China Carbon Trading Market[77]. The price is *USD* 8.00/ton.

Market research and statistics were conducted on the price of EPS polystyrene foam board, a variable parameter building material involved in exterior walls, and It was concluded that the price of EPS polystyrene foam board in Jilin Province is 23 USD/m^3[78]. It was concluded that the price of EPS polystyrene foam board in Liaoning Province is 22 USD/m^3[79]. It was

concluded that the price of EPS polystyrene foam board in Shanxi Province is 21 USD/m^3[80]. The cost of exterior wall renovation is shown in Table 17. Exterior wall renovation cost list.

Market research and statistics were conducted on the price of EPS polystyrene foam board, a variable parameter building material involved in roof, and It was concluded that the price of EPS polystyrene foam board in Jilin Province is 23 USD/m^3[78]. It was concluded that the price of EPS polystyrene foam board in Liaoning Province is 22 USD/m^3[79]. It was concluded that the price of EPS polystyrene foam board in Shanxi Province is 21 USD/m^3[80]. The cost of exterior wall renovation is shown in Table 18. Roof renovation cost list.

Market research and statistics were conducted on the prices of exterior windows involved in the study[73]. The cost of exterior window renovation is shown in Table 19. Exterior window renovation cost list.

The net present value results are shown in Figure 23.

The static and discounted investment payback periods of all 17 experimental groups in Changchun City are less than 50 years, so all 17 experimental groups are feasible. Because the parameter selection of the orthogonal analysis is based on the impact of the parameters on carbon emissions, and the parameter selection is not based on the economic impact, among the 17 groups of plans, the most recommended design plan in the economic direction is plan16: A4B4C1, 85 mm EPS polystyrene foam board (A4), 100 *mm* EPS polystyrene foam board (B4), Plastic steel frame and triple glass window 3+11(A)+3 single silver Low-e+11(Ar)+3(C1). The annual carbon emissions are 95.62t, and the carbon dioxide emission reduction rate is 19.44%. The static investment payback period is 2.51 years. The discounted investment payback period is 2.72 years, and the net present value is USD 9475.4.

The static and discounted investment payback periods of all 17 experimental groups in Shenyang City are less than 50 years, so all 17 experimental groups are feasible. Because the parameter selection of the orthogonal analysis is based on the impact of the parameters on carbon emissions, and the parameter selection is not based on the economic impact, among the 17 groups of plans, the most recommended design plan in the economic direction is plan16: A4B4C1, 85 mm EPS polystyrene foam board

(A4), 100 *mm* EPS polystyrene foam board (B4), Plastic steel frame and triple glass window 3+11(A)+3 single silver Low-e+11(Ar)+3 (C1). The annual carbon emissions are 92.64t, and the carbon dioxide emission reduction rate is 10.24%. The static investment payback period is 3.1 years. The discounted investment payback period is 3.43 years, and the net present value is USD 9222.1.

The static and discounted investment payback periods of all 17 experimental groups in Datong City are less than 50 years, so all 17 experimental groups are feasible. Because the parameter selection of the orthogonal analysis is based on the impact of the parameters on carbon emissions, and the parameter selection is not based on the economic impact, among the 17 groups of plans, the most recommended design plan in the economic direction is plan16: A4B4C1, 85 mm EPS polystyrene foam board (A4), 100 *mm* EPS polystyrene foam board (B4), Plastic steel frame and triple glass window 3+11(A)+3 single silver Low-e+11(Ar)+3 (C1). The annual carbon emissions are 93.44 t, and the carbon dioxide emission reduction rate is 13.35%. The static investment payback period is 4.2 years. The discounted investment payback period is 4.51 years and the net present value is USD 9012.3.

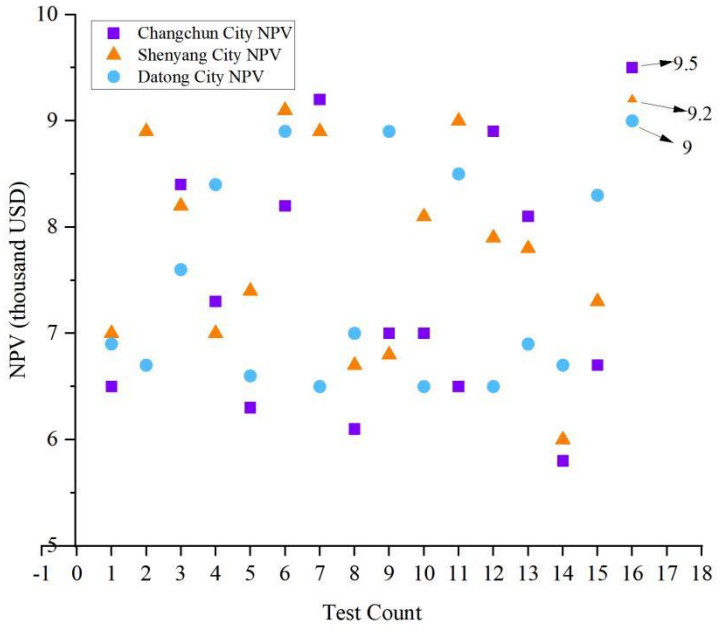

Figure 23. Net present value.

Table 17. Exterior wall renovation cost list

Modification materials	Material quantity	Labor cost	Machinery cost	Total cost in Changchun City	Total cost in Shenyang City	Total cost in Datong City
65mm EPS polystyrene foam board	135.4m^3	4.4 USD/m^3	0.4 USD/m^3	3764.12USD	3628.72USD	3493.32USD
70mm EPS polystyrene foam board	145.8m^3	4.4 USD/m^3	0.4 USD/m^3	4053.24USD	3907.44USD	3761.64USD
75mm EPS polystyrene foam board	156.2m^3	4.4 USD/m^3	0.4 USD/m^3	4229.90USD	4186.16USD	4029.96USD
80mm EPS polystyrene foam board	166.7m^3	4.4 USD/m^3	0.4 USD/m^3	4634.26USD	4467.56USD	4300.86USD
85mm EPS polystyrene foam board	177.1m^3	4.4 USD/m^3	0.4 USD/m^3	4923.38USD	4746.28USD	4569.18USD

Table 18. Roof renovation cost list

Modification materials	Material quantity	Labor cost	Machinery cost	Total cost in Changchun City	Total cost in Shenyang City	Total cost in Datong City
55mm EPS polystyrene foam board	26.5m^3	4.9 USD/m^3	0.4 USD/m^3	749.95 USD	723.45 USD	696.95 USD
60mm EPS polystyrene foam board	28.9m^3	4.9 USD/m^3	0.4 USD/m^3	817.87 USD	788.97 USD	760.07 USD
65mm EPS polystyrene foam board	31.3m^3	4.9 USD/m^3	0.4 USD/m^3	885.79 USD	854.49 USD	823.19 USD
70mm EPS polystyrene foam board	33.7m^3	4.9 USD/m^3	0.4 USD/m^3	953.71 USD	920.01 USD	886.31 USD
75mm EPS polystyrene foam board	36.1m^3	4.9 USD/m^3	0.4 USD/m^3	1021.63 USD	985.53 USD	949.43 USD
80mm EPS polystyrene foam board	38.5m^3	4.9 USD/m^3	0.4 USD/m^3	1089.55 USD	1051.05 USD	1012.55 USD
85mm EPS polystyrene foam board	40.9m^3	4.9 USD/m^3	0.4 USD/m^3	1157.47 USD	1116.57 USD	1075.67 USD
90mm EPS polystyrene foam board	43.3m^3	4.9 USD/m^3	0.4 USD/m^3	1225.39 USD	1182.09 USD	1138.79 USD
95mm EPS polystyrene foam board	45.7m^3	4.9 USD/m^3	0.4 USD/m^3	1293.31 USD	1247.61 USD	1201.91 USD
100mm EPS polystyrene foam board	48.1m^3	4.9 USD/m^3	0.4 USD/m^3	1361.23 USD	1313.13 USD	1265.03 USD

Table 19. Exterior window renovation cost list.

Exterior window	Material quantity	Labor cost	Machinery cost	Material cost	Total cost
MP16 = Plastic steel frame and triple glass window 5 + 9(A) + 4 single silver Low-e + 12 (Ar) + 5	145m^2	5.2 USD/m^2	0.8 USD/m^2	59.2 USD/m^2	12573 USD
MP17 = Plastic steel frame and triple glass window 3 + 11(A) + 3 double silver Low-e + 11 (Ar) + 3	145m^2	5.2 USD/m^2	0.8 USD/m^2	74.4 USD/m^2	11658 USD
MP18 = Plastic steel frame and triple glass window 4 + 10(A) + 4 double silver Low-e + 10 (Ar) + 4	145m^2	5.2 USD/m^2	0.8 USD/m^2	89.7 USD/m^2	13876.5 USD
MP19 = Plastic steel frame and double glass window 6 + Vacuum+ 6 single silver Low-e	145m^2	5.2 USD/m^2	0.8 USD/m^2	100.7 USD/m^2	15471.5 USD
MP20 = Plastic steel frame and triple glass window 6 + Vacuum + 6 double silver Low-e + PolyVinyl Butyral Film + 6	145m^2	5.2 USD/m^2	0.8 USD/m^2	118.3 USD/m^2	18023.5 USD

6.5.1. Sensitivity Analysis

The sensitivity analysis aims at the robustness of the findings and discusses the influence of other elements on the results. Because this chapter focuses on economic analysis, a sensitivity analysis of the uncertainty factors affecting the net present value was performed. The three variables considered in the calculation of net present value in this paper are annual cost savings (*CI*), the initial investment cost (*CO*), and the discount rate. Because the initial investment cost only exists for the first year, this study performs a two-factor sensitivity analysis on the two major sensitivity factors, cost savings and discount rate, to evaluate the potential changes in various uncertainty elements in the project reality.

Assuming that the percentage change in incremental cost is x and the value of change in the discount rate is r, according to Equation (14), the net present value is

$$NPV = -CI(1-x) + CO\frac{(1+r)^{50}-1}{r(1+r)^{50}} \qquad (14)$$

The values of *CI* and *CO* were taken as obtained in the above calculation.

When net present value is equal to 0, 17 equations are obtained with r values of 1%, 2%, 3%, 4%, 5% ... 19%, 20%, the corresponding x-value statistics in Changchun City are shown in Table 17, and the function curves are plotted as shown in Figure 24. The corresponding x-value statistics in Shengyang City are shown in Table 18, and the function curves are plotted as shown in Figure 25. The corresponding x-value statistics in Datong City are shown in Table 19, and the function curves are plotted as shown in Figure 26.

Each point on the 51 curves corresponding to *(r, x)* makes the net present value equal to 0 as the critical line. If the net present value at any point in the upper left region of the curve is greater than 0, the project is economically feasible; if the net present value at any point in the lower right region is less than 0, the project is economically infeasible.

As can be seen from the data in Table 16-18, when the discount rate changes, it is guaranteed that the project remains economically feasible as

long as the rate of change of the actual cost savings is greater than the x-limit value corresponding to the value of *r* in the table.

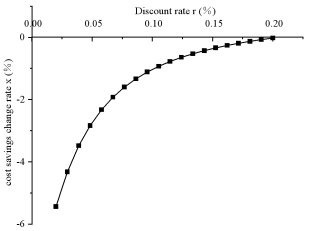

(**a**) Function (1)

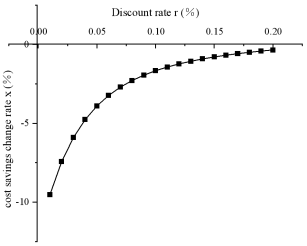

(**b**) Function (2)

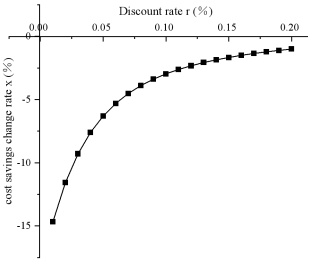

(**c**) Function (3)

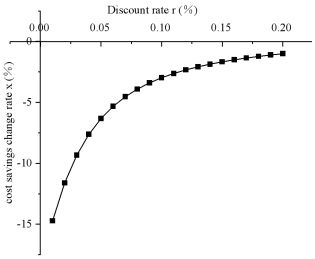

(**d**) Function (4)

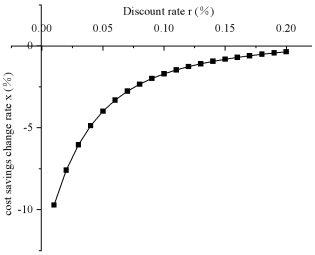

(**e**) Function (5)

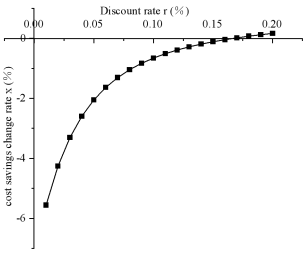

(**f**) Function (6)

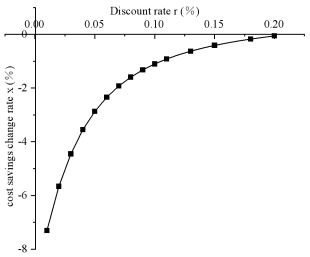

(**g**) Function (7)

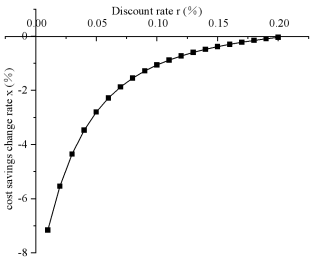

(**h**) Function (8)

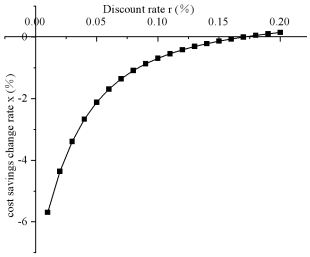

(**i**) Function (9)

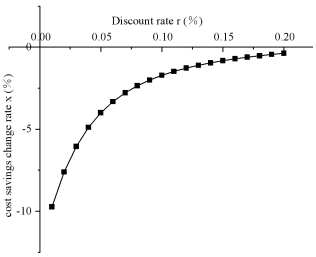

(**j**) Function (10)

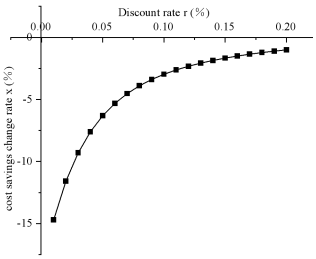

(**k**) Function (11)

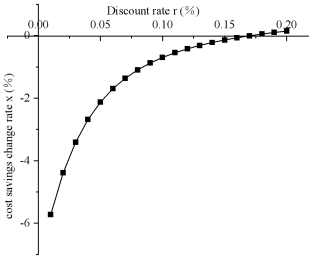

(**l**) Function (12)

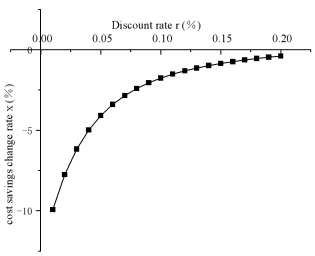

(**m**) Function (13)

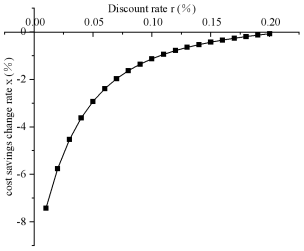

(**n**) Function (14)

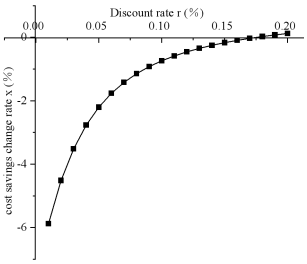

(**o**) Function (15)

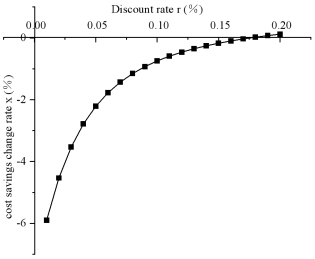

(**p**) Function (16)

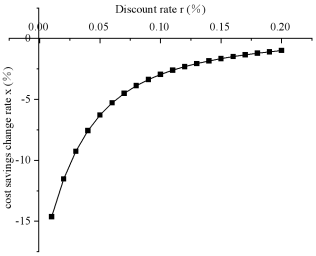

(**q**) Function (17)

Figure 24. Two-factor sensitivity incremental cost and discount rate analysis graph in Changchun City.

Table 17. Table of limiting values of the corresponding cost savings change rates at different discount rates in Changchun City.

	Function (1) $x = 1 - 0.3998 * [(1 + r)^{50} - 1]/[r * (1 + r)^{50}]$									
r	1%	2%	3%	4%	5%	6%	7%	8%	9%	10%
x	−14.67	−11.56	−9.29	−7.59	−6.30	−5.30	−4.52	−3.89	−3.38	−2.96
r	11%	12%	13%	14%	15%	16%	17%	18%	19%	20%
x	−2.61	−2.32	−2.07	−1.85	−1.66	−1.50	−1.35	−1.22	−1.10	−1.00
	Function (2) $x = 1 - 0.2684 * [(1 + r)^{50} - 1]/[r * (1 + r)^{50}]$									
r	1%	2%	3%	4%	5%	6%	7%	8%	9%	10%
x	−9.52	−7.43	−5.92	−4.77	−3.90	−3.23	−2.70	−2.28	−1.94	−1.66
r	11%	12%	13%	14%	15%	16%	17%	18%	19%	20%
x	−1.43	−1.23	−1.06	−0.91	−0.79	−0.68	−0.58	−0.49	−0.41	−0.34
	Function (3) $x = 1 - 0.2048 * [(1 + r)^{50} - 1]/[r * (1 + r)^{50}]$									
r	1%	2%	3%	4%	5%	6%	7%	8%	9%	10%
x	−7.03	−5.44	−4.27	−3.40	−2.74	−2.23	−1.83	−1.51	−1.24	−1.03
r	11%	12%	13%	14%	15%	16%	17%	18%	19%	20%
x	−0.85	−0.70	−0.57	−0.46	−0.36	−0.28	−0.20	−0.14	−0.08	−0.02
	Function (4) $x = 1 - 0.1673 * [(1 + r)^{50} - 1]/[r * (1 + r)^{50}]$									
r	1%	2%	3%	4%	5%	6%	7%	8%	9%	10%
x	−5.56	−4.26	−3.30	−2.59	−2.05	−1.64	−1.31	−1.05	−0.83	−0.66
r	11%	12%	13%	14%	15%	16%	17%	18%	19%	20%
x	−0.51	−0.39	−0.28	−0.19	−0.11	−0.04	0.02	0.07	0.12	0.16
	Function (5) $x = 1 - 0.2734 * [(1 + r)^{50} - 1]/[r * (1 + r)^{50}]$									
r	1%	2%	3%	4%	5%	6%	7%	8%	9%	10%
x	−9.72	−7.59	−6.03	−4.87	−3.99	−3.31	−2.77	−2.34	−2.00	−1.71
r	11%	12%	13%	14%	15%	16%	17%	18%	19%	20%
x	−1.47	−1.27	−1.10	−0.95	−0.82	−0.71	−0.61	−0.52	−0.44	−0.37
	Function (6) $x = 1 - 0.4011 * [(1 + r)^{50} - 1]/[r * (1 + r)^{50}]$									
r	1%	2%	3%	4%	5%	6%	7%	8%	9%	10%
x	−14.72	−11.60	−9.32	−7.62	−6.33	−5.32	−4.54	−3.91	−3.40	−2.98
r	11%	12%	13%	14%	15%	16%	17%	18%	19%	20%
x	−2.63	−2.33	−2.08	−1.86	−1.67	−1.51	−1.36	−1.23	−1.11	−1.01
	Function (7) $x = 1 - 0.1707 * [(1 + r)^{50} - 1]/[r * (1 + r)^{50}]$									
r	1%	2%	3%	4%	5%	6%	7%	8%	9%	10%
x	−5.69	−4.36	−3.39	−2.67	−2.12	−1.69	−1.36	−1.09	−0.87	−0.69
r	11%	12%	13%	14%	15%	16%	17%	18%	19%	20%
x	−0.54	−0.42	−0.31	−0.22	−0.14	−0.07	0.00	0.05	0.10	0.15
	Function (8) $x = 1 - 0.2081 * [(1 + r)^{50} - 1]/[r * (1 + r)^{50}]$									
r	1%	2%	3%	4%	5%	6%	7%	8%	9%	10%
x	−7.16	−5.54	−4.35	−3.47	−2.80	−2.28	−1.87	−1.55	−1.28	−1.06
r	11%	12%	13%	14%	15%	16%	17%	18%	19%	20%
x	−0.88	−0.73	−0.60	−0.48	−0.39	−0.30	−0.22	−0.16	−0.10	−0.04
	Function (9) $x = 1 - 0.2119 * [(1 + r)^{50} - 1]/[r * (1 + r)^{50}]$									
r	1%	2%	3%	4%	5%	6%	7%	8%	9%	10%
x	−7.31	−5.66	−4.45	−3.55	−2.87	−2.34	−1.92	−1.59	−1.32	−1.10
r	11%	12%	13%	14%	15%	16%	17%	18%	19%	20%
x	−0.92	−0.76	−0.63	−0.51	0.41	0.32	−0.25	−0.18	−0.12	−0.06
	Function (10) $x = 1 - 0.1714 * [(1 + r)^{50} - 1]/[r * (1 + r)^{50}]$									
r	1%	2%	3%	4%	5%	6%	7%	8%	9%	10%
x	−5.72	−4.39	−3.41	−2.68	−2.13	−1.70	−1.37	−1.10	−0.88	−0.70
r	11%	12%	13%	14%	15%	16%	17%	18%	19%	20%
x	−0.55	−0.42	−0.32	−0.22	−0.14	−0.07	−0.01	0.05	0.10	0.14
	Function (11) $x = 1 - 0.4006 * [(1 + r)^{50} - 1]/[r * (1 + r)^{50}]$									
r	1%	2%	3%	4%	5%	6%	7%	8%	9%	10%
x	−14.70	−11.59	−9.31	−7,61	−6.31	−5.31	−4.53	−3.90	−3.39	2.97
r	11%	12%	13%	14%	15%	16%	17%	18%	19%	20%
x	−2.62	−2.33	−2.07	−1.86	−1.67	−1.50	−1.36	−1.22	−1.11	−1.00
	Function (12) $x = 1 - 0.2739 * [(1 + r)^{50} - 1]/[r * (1 + r)^{50}]$									
r	1%	2%	3%	4%	5%	6%	7%	8%	9%	10%
x	−9,74	7.61	−6.05	−4.88	−4.00	−3.32	−2.78	−2.35	−2.00	−1.72
r	11%	12%	13%	14%	15%	16%	17%	18%	19%	20%
x	−1.48	−1.27	−1.10	−0.95	−0.82	−0.71	−0.61	−0.52	−0.44	−0.37

	Function (13) $x = 1 - 0.1755 * [(1 + r)^{50} - 1]/[r * (1 + r)^{50}]$									
r	1%	2%	3%	4%	5%	6%	7%	8%	9%	10%
x	−5.88	−4.51	−3.52	−2.77	−2.20	−1.77	−1.42	−1.15	−0.92	−0.74
r	11%	12%	13%	14%	15%	16%	17%	18%	19%	20%
x	−0.59	−0.46	−0.35	−0.25	−0.17	−0.10	−0.03	−0.02	0.08	0.12
	Function (14) $x = 1 - 0.2151 * [(1 + r)^{50} - 1]/[r * (1 + r)^{50}]$									
r	1%	2%	3%	4%	5%	6%	7%	8%	9%	10%
x	−7.43	−5.76	−4.53	−3.62	−2.93	−2.39	−1.97	−1.63	−1.36	−1.13
r	11%	12%	13%	14%	15%	16%	17%	18%	19%	20%
x	−0.94	−0.79	−0.65	−0.53	−0.43	−0.34	−0.26	−0.19	−0.13	−0.08
	Function (15) $x = 1 - 0.2788 * [(1 + r)^{50} - 1]/[r * (1 + r)^{50}]$									
r	1%	2%	3%	4%	5%	6%	7%	8%	9%	10%
x	−9.93	−7.76	−6.17	−4.99	−4.09	−3.39	−2.85	−2.41	−2.06	−1.76
r	11%	12%	13%	14%	15%	16%	17%	18%	19%	20%
x	−1.52	−1.31	−1.14	−0.99	−0.86	−0.74	−0.64	−0.55	−0.47	−0.39
	Function (16) $x = 1 - 0.3988 * [(1 + r)^{50} - 1]/[r * (1 + r)^{50}]$									
r	1%	2%	3%	4%	5%	6%	7%	8%	9%	10%
x	−14.63	−11.53	−9.26	−7.57	−6.28	−5.29	−4.50	−3.88	−3.37	−2.95
r	11%	12%	13%	14%	15%	16%	17%	18%	19%	20%
x	−2.61	−2.31	−2.06	−1.84	−1.66	−1.49	−1.34	−1.21	−1.10	−0.99
	Function (17) $x = 1 - 0.1761 * [(1 + r)^{50} - 1]/[r * (1 + r)^{50}]$									
r	1%	2%	3%	4%	5%	6%	7%	8%	9%	10%
x	−5.90	−4.53	−3.53	−2.78	−2.21	−1.78	−1.43	−1.15	−0.93	−0.75
r	11%	12%	13%	14%	15%	16%	17%	18%	19%	20%
x	−0.59	−0.46	−0.35	−0.26	−0.17	−0.10	−0.04	0.02	0.07	0.12

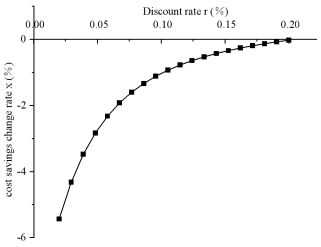

(**a**) Function (1)

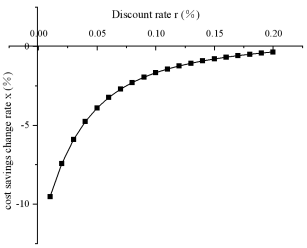

(**b**) Function (2)

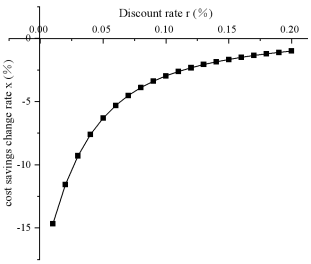

(**c**) Function (3)

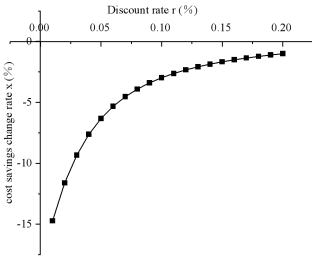

(**d**) Function (4)

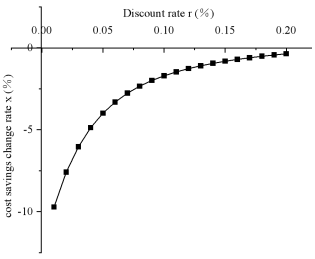

(**e**) Function (5)

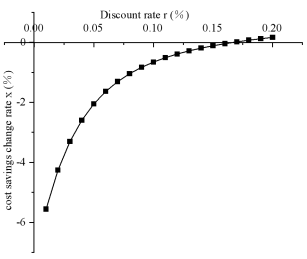

(**f**) Function (6)

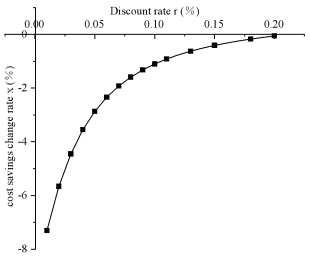

(**g**) Function (7)

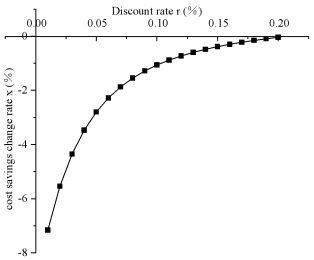

(**h**) Function (8)

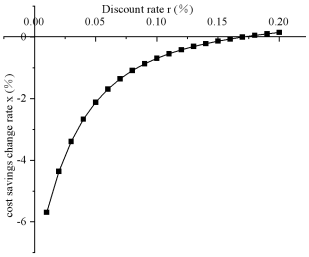

(**i**) Function (9)

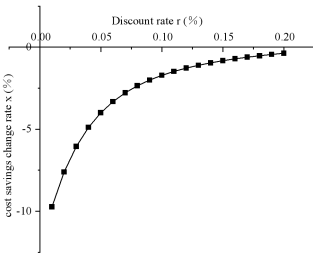

(**j**) Function (10)

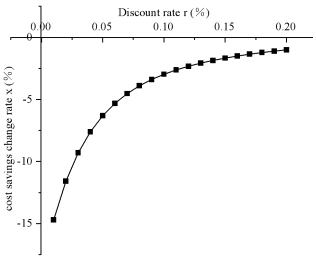

(**k**) Function (11)

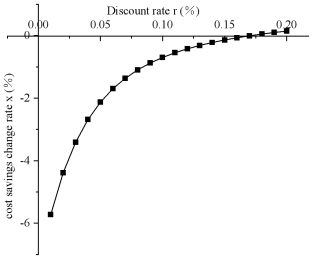

(**l**) Function (12)

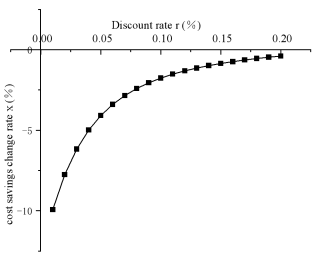

(**m**) Function (13)

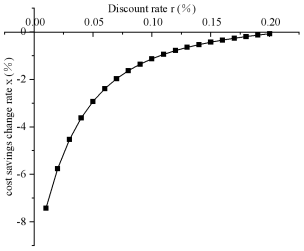

(**n**) Function (14)

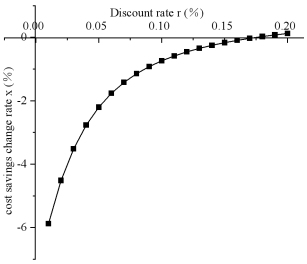

(**o**) Function (15)

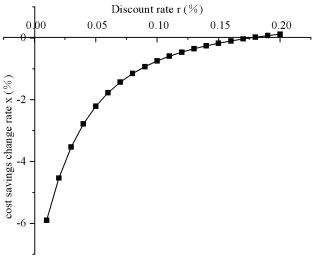

(**p**) Function (16)

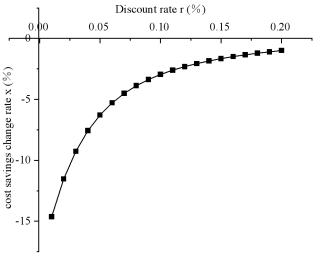

(**q**) Function (17)

Figure 25. Two-factor sensitivity incremental cost and discount rate analysis graph in Shenyang City.

Table 18. Table of limiting values of the corresponding cost savings change rates at different discount rates in Shenyang City.

Function (1) $x = 1 - 0.28498 * [(1 + r)^{50} - 1]/[r * (1 + r)^{50}]$										
r	1%	2%	3%	4%	5%	6%	7%	8%	9%	10%
x	−14.67	−11.56	−9.29	−7.59	−6.30	−5.30	−4.52	−3.89	−3.38	−2.96
r	11%	12%	13%	14%	15%	16%	17%	18%	19%	20%
x	−2.61	−2.32	−2.07	−1.85	−1.66	−1.50	−1.35	−1.22	−1.10	−1.00
Function (2) $x = 1 - 0.29354 * [(1 + r)^{50} - 1]/[r * (1 + r)^{50}]$										
r	1%	2%	3%	4%	5%	6%	7%	8%	9%	10%
x	−9.52	−7.43	−5.92	−4.77	−3.90	−3.23	−2.70	−2.28	−1.94	−1.66
r	11%	12%	13%	14%	15%	16%	17%	18%	19%	20%
x	−1.43	−1.23	−1.06	−0.91	−0.79	−0.68	−0.58	−0.49	−0.41	−0.34
Function (3) $x = 1 - 0.19728 * [(1 + r)^{50} - 1]/[r * (1 + r)^{50}]$										
r	1%	2%	3%	4%	5%	6%	7%	8%	9%	10%
x	−7.03	−5.44	−4.27	−3.40	−2.74	−2.23	−1.83	−1.51	−1.24	−1.03
r	11%	12%	13%	14%	15%	16%	17%	18%	19%	20%
x	−0.85	−0.70	−0.57	−0.46	−0.36	−0.28	−0.20	−0.14	−0.08	−0.02
Function (4) $x = 1 - 0.18343 * [(1 + r)^{50} - 1]/[r * (1 + r)^{50}]$										
r	1%	2%	3%	4%	5%	6%	7%	8%	9%	10%
x	−5.56	−4.26	−3.30	−2.59	−2.05	−1.64	−1.31	−1.05	−0.83	−0.66
r	11%	12%	13%	14%	15%	16%	17%	18%	19%	20%
x	−0.51	−0.39	−0.28	−0.19	−0.11	−0.04	0.02	0.07	0.12	0.16
Function (5) $x = 1 - 0.2254 * [(1 + r)^{50} - 1]/[r * (1 + r)^{50}]$										
r	1%	2%	3%	4%	5%	6%	7%	8%	9%	10%
x	−9.72	−7.59	−6.03	−4.87	−3.99	−3.31	−2.77	−2.34	−2.00	−1.71
r	11%	12%	13%	14%	15%	16%	17%	18%	19%	20%
x	−1.47	−1.27	−1.10	−0.95	−0.82	−0.71	−0.61	−0.52	−0.44	−0.37
Function (6) $x = 1 - 0.3941 * [(1 + r)^{50} - 1]/[r * (1 + r)^{50}]$										
r	1%	2%	3%	4%	5%	6%	7%	8%	9%	10%
x	−14.72	−11.60	−9.32	−7.62	−6.33	−5.32	−4.54	−3.91	−3.40	−2.98
r	11%	12%	13%	14%	15%	16%	17%	18%	19%	20%
x	−2.63	−2.33	−2.08	−1.86	−1.67	−1.51	−1.36	−1.23	−1.11	−1.01
Function (7) $x = 1 - 0.1327 * [(1 + r)^{50} - 1]/[r * (1 + r)^{50}]$										
r	1%	2%	3%	4%	5%	6%	7%	8%	9%	10%
x	−5.69	−4.36	−3.39	−2.67	−2.12	−1.69	−1.36	−1.09	−0.87	−0.69
r	11%	12%	13%	14%	15%	16%	17%	18%	19%	20%
x	−0.54	−0.42	−0.31	−0.22	−0.14	−0.07	0.00	0.05	0.10	0.15
Function (8) $x = 1 - 0.2121 * [(1 + r)^{50} - 1]/[r * (1 + r)^{50}]$										
r	1%	2%	3%	4%	5%	6%	7%	8%	9%	10%
x	−7.16	−5.54	−4.35	−3.47	−2.80	−2.28	−1.87	−1.55	−1.28	−1.06
r	11%	12%	13%	14%	15%	16%	17%	18%	19%	20%
x	−0.88	−0.73	−0.60	−0.48	−0.39	−0.30	−0.22	−0.16	−0.10	−0.04
Function (9) $x = 1 - 0.1919 * [(1 + r)^{50} - 1]/[r * (1 + r)^{50}]$										
r	1%	2%	3%	4%	5%	6%	7%	8%	9%	10%
x	−7.31	−5.66	−4.45	−3.55	−2.87	−2.34	−1.92	−1.59	−1.32	−1.10
r	11%	12%	13%	14%	15%	16%	17%	18%	19%	20%
x	−0.92	−0.76	−0.63	−0.51	0.41	0.32	−0.25	−0.18	−0.12	−0.06
Function (10) $x = 1 - 0.1714 * [(1 + r)^{50} - 1]/[r * (1 + r)^{50}]$										
r	1%	2%	3%	4%	5%	6%	7%	8%	9%	10%
x	−5.72	−4.39	−3.41	−2.68	−2.13	−1.70	−1.37	−1.10	−0.88	−0.70
r	11%	12%	13%	14%	15%	16%	17%	18%	19%	20%
x	−0.55	−0.42	−0.32	−0.22	−0.14	−0.07	−0.01	0.05	0.10	0.14
Function (11) $x = 1 - 0.3806 * [(1 + r)^{50} - 1]/[r * (1 + r)^{50}]$										
r	1%	2%	3%	4%	5%	6%	7%	8%	9%	10%
x	−14.70	−11.59	−9.31	−7,61	−6.31	−5.31	−4.53	−3.90	−3.39	2.97
r	11%	12%	13%	14%	15%	16%	17%	18%	19%	20%
x	−2.62	−2.33	−2.07	−1.86	−1.67	−1.50	−1.36	−1.22	−1.11	−1.00
Function (12) $x = 1 - 0.2739 * [(1 + r)^{50} - 1]/[r * (1 + r)^{50}]$										
r	1%	2%	3%	4%	5%	6%	7%	8%	9%	10%
x	−9,74	7.61	−6.05	−4.88	−4.00	−3.32	−2.78	−2.35	−2.00	−1.72
r	11%	12%	13%	14%	15%	16%	17%	18%	19%	20%
x	−1.48	−1.27	−1.10	−0.95	−0.82	−0.71	−0.61	−0.52	−0.44	−0.37

	Function (13) $x = 1 - 0.1695 * [(1 + r)^{50} - 1]/[r * (1 + r)^{50}]$									
r	1%	2%	3%	4%	5%	6%	7%	8%	9%	10%
x	−5.88	−4.51	−3.52	−2.77	−2.20	−1.77	−1.42	−1.15	−0.92	−0.74
r	11%	12%	13%	14%	15%	16%	17%	18%	19%	20%
x	−0.59	−0.46	−0.35	−0.25	−0.17	−0.10	−0.03	−0.02	0.08	0.12
	Function (14) $x = 1 - 0.2051 * [(1 + r)^{50} - 1]/[r * (1 + r)^{50}]$									
r	1%	2%	3%	4%	5%	6%	7%	8%	9%	10%
x	−7.43	−5.76	−4.53	−3.62	−2.93	−2.39	−1.97	−1.63	−1.36	−1.13
r	11%	12%	13%	14%	15%	16%	17%	18%	19%	20%
x	−0.94	−0.79	−0.65	−0.53	−0.43	−0.34	−0.26	−0.19	−0.13	−0.08
	Function (15) $x = 1 - 0.1988 * [(1 + r)^{50} - 1]/[r * (1 + r)^{50}]$									
r	1%	2%	3%	4%	5%	6%	7%	8%	9%	10%
x	−9.93	−7.76	−6.17	−4.99	−4.09	−3.39	−2.85	−2.41	−2.06	−1.76
r	11%	12%	13%	14%	15%	16%	17%	18%	19%	20%
x	−1.52	−1.31	−1.14	−0.99	−0.86	−0.74	−0.64	−0.55	−0.47	−0.39
	Function (16) $x = 1 - 0.3428 * [(1 + r)^{50} - 1]/[r * (1 + r)^{50}]$									
r	1%	2%	3%	4%	5%	6%	7%	8%	9%	10%
x	−14.63	−11.53	−9.26	−7.57	−6.28	−5.29	−4.50	−3.88	−3.37	−2.95
r	11%	12%	13%	14%	15%	16%	17%	18%	19%	20%
x	−2.61	−2.31	−2.06	−1.84	−1.66	−1.49	−1.34	−1.21	−1.10	−0.99
	Function (17) $x = 1 - 0.1561 * [(1 + r)^{50} - 1]/[r * (1 + r)^{50}]$									
r	1%	2%	3%	4%	5%	6%	7%	8%	9%	10%
x	−5.90	−4.53	−3.53	−2.78	−2.21	−1.78	−1.43	−1.15	−0.93	−0.75
r	11%	12%	13%	14%	15%	16%	17%	18%	19%	20%
x	−0.59	−0.46	−0.35	−0.26	−0.17	−0.10	−0.04	0.02	0.07	0.12

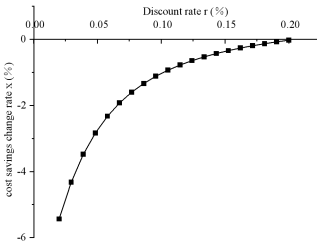

(**a**) Function (1)

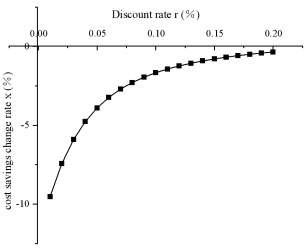

(**b**) Function (2)

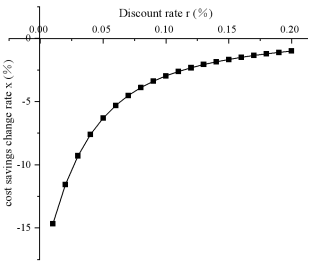

(**c**) Function (3)

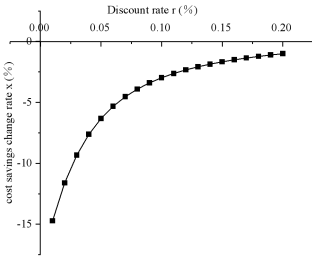

(**d**) Function (4)

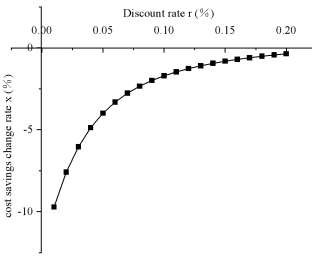

(**e**) Function (5)

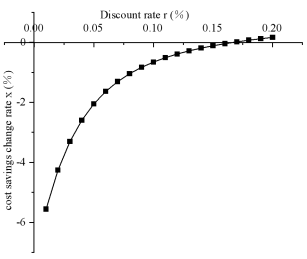

(**f**) Function (6)

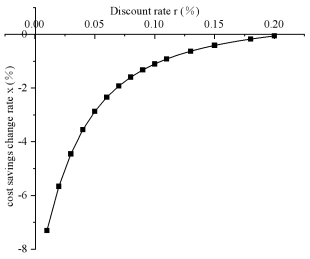

(**g**) Function (7)

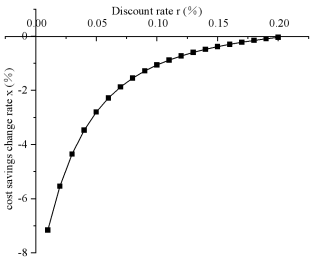

(**h**) Function (8)

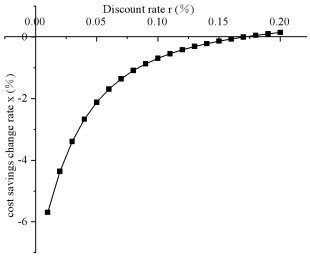

(**i**) Function (9)

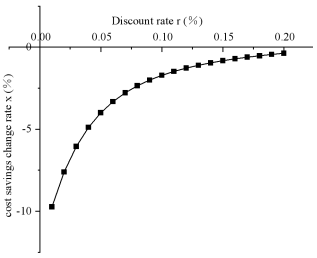

(**j**) Function (10)

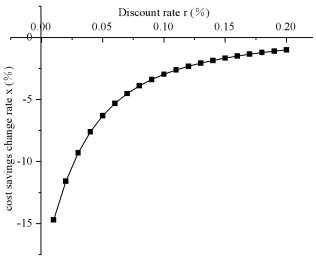

(**k**) Function (11)

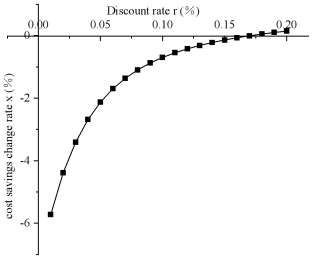

(**l**) Function (12)

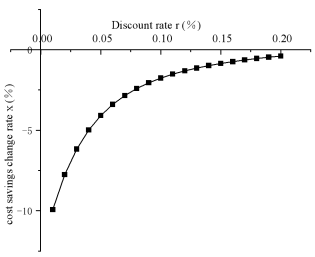

(**m**) Function (13)

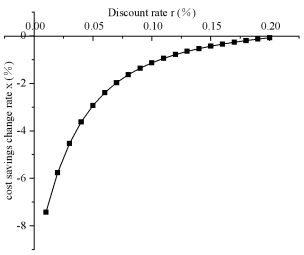

(**n**) Function (14)

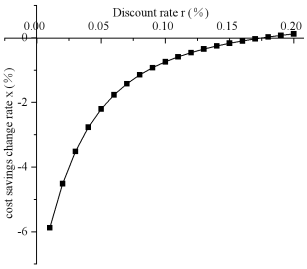

(**o**) Function (15)

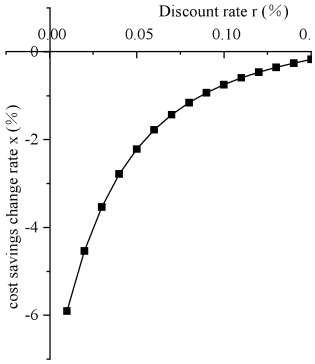

(**p**) Function (16)

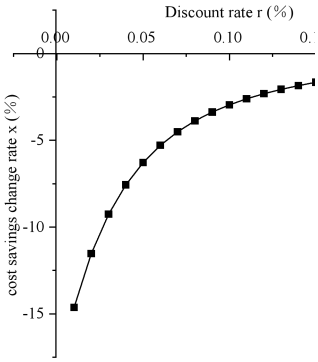

(**q**) Function (17)

Figure 26. Two-factor sensitivity incremental cost and discount rate analysis graph in Datong City.

Table 19. Table of limiting values of the corresponding cost savings change rates at different discount rates in Datong City.

	Function (1) $x = 1 - 0.248 * [(1 + r)^{50} - 1]/[r * (1 + r)^{50}]$									
r	1%	2%	3%	4%	5%	6%	7%	8%	9%	10%
x	−14.67	−11.56	−9.29	−7.59	−6.30	−5.30	−4.52	−3.89	−3.38	−2.96
r	11%	12%	13%	14%	15%	16%	17%	18%	19%	20%
x	−2.61	−2.32	−2.07	−1.85	−1.66	−1.50	−1.35	−1.22	−1.10	−1.00
	Function (2) $x = 1 - 0.1974 * [(1 + r)^{50} - 1]/[r * (1 + r)^{50}]$									
r	1%	2%	3%	4%	5%	6%	7%	8%	9%	10%
x	−9.52	−7.43	−5.92	−4.77	−3.90	−3.23	−2.70	−2.28	−1.94	−1.66
r	11%	12%	13%	14%	15%	16%	17%	18%	19%	20%
x	−1.43	−1.23	−1.06	−0.91	−0.79	−0.68	−0.58	−0.49	−0.41	−0.34
	Function (3) $x = 1 - 0.2588 * [(1 + r)^{50} - 1]/[r * (1 + r)^{50}]$									
r	1%	2%	3%	4%	5%	6%	7%	8%	9%	10%
x	−7.03	−5.44	−4.27	−3.40	−2.74	−2.23	−1.83	−1.51	−1.24	−1.03
r	11%	12%	13%	14%	15%	16%	17%	18%	19%	20%
x	−0.85	−0.70	−0.57	−0.46	−0.36	−0.28	−0.20	−0.14	−0.08	−0.02
	Function (4) $x = 1 - 0.2073 * [(1 + r)^{50} - 1]/[r * (1 + r)^{50}]$									
r	1%	2%	3%	4%	5%	6%	7%	8%	9%	10%
x	−5.56	−4.26	−3.30	−2.59	−2.05	−1.64	−1.31	−1.05	−0.83	−0.66
r	11%	12%	13%	14%	15%	16%	17%	18%	19%	20%
x	−0.51	−0.39	−0.28	−0.19	−0.11	−0.04	0.02	0.07	0.12	0.16
	Function (5) $x = 1 - 0.2534 * [(1 + r)^{50} - 1]/[r * (1 + r)^{50}]$									
r	1%	2%	3%	4%	5%	6%	7%	8%	9%	10%
x	−9.72	−7.59	−6.03	−4.87	−3.99	−3.31	−2.77	−2.34	−2.00	−1.71
r	11%	12%	13%	14%	15%	16%	17%	18%	19%	20%
x	−1.47	−1.27	−1.10	−0.95	−0.82	−0.71	−0.61	−0.52	−0.44	−0.37
	Function (6) $x = 1 - 0.3921 * [(1 + r)^{50} - 1]/[r * (1 + r)^{50}]$									
r	1%	2%	3%	4%	5%	6%	7%	8%	9%	10%
x	−14.72	−11.60	−9.32	−7.62	−6.33	−5.32	−4.54	−3.91	−3.40	−2.98
r	11%	12%	13%	14%	15%	16%	17%	18%	19%	20%
x	−2.63	−2.33	−2.08	−1.86	−1.67	−1.51	−1.36	−1.23	−1.11	−1.01
	Function (7) $x = 1 - 0.2903 * [(1 + r)^{50} - 1]/[r * (1 + r)^{50}]$									
r	1%	2%	3%	4%	5%	6%	7%	8%	9%	10%
x	−5.69	−4.36	−3.39	−2.67	−2.12	−1.69	−1.36	−1.09	−0.87	−0.69
r	11%	12%	13%	14%	15%	16%	17%	18%	19%	20%
x	−0.54	−0.42	−0.31	−0.22	−0.14	−0.07	0.00	0.05	0.10	0.15
	Function (8) $x = 1 - 0.2231 * [(1 + r)^{50} - 1]/[r * (1 + r)^{50}]$									
r	1%	2%	3%	4%	5%	6%	7%	8%	9%	10%
x	−7.16	−5.54	−4.35	−3.47	−2.80	−2.28	−1.87	−1.55	−1.28	−1.06
r	11%	12%	13%	14%	15%	16%	17%	18%	19%	20%
x	−0.88	−0.73	−0.60	−0.48	−0.39	−0.30	−0.22	−0.16	−0.10	−0.04
	Function (9) $x = 1 - 0.1923 * [(1 + r)^{50} - 1]/[r * (1 + r)^{50}]$									
r	1%	2%	3%	4%	5%	6%	7%	8%	9%	10%
x	−7.31	−5.66	−4.45	−3.55	−2.87	−2.34	−1.92	−1.59	−1.32	−1.10
r	11%	12%	13%	14%	15%	16%	17%	18%	19%	20%
x	−0.92	−0.76	−0.63	−0.51	0.41	0.32	−0.25	−0.18	−0.12	−0.06
	Function (10) $x = 1 - 0.1832 * [(1 + r)^{50} - 1]/[r * (1 + r)^{50}]$									
r	1%	2%	3%	4%	5%	6%	7%	8%	9%	10%
x	−5.72	−4.39	−3.41	−2.68	−2.13	−1.70	−1.37	−1.10	−0.88	−0.70
r	11%	12%	13%	14%	15%	16%	17%	18%	19%	20%
x	−0.55	−0.42	−0.32	−0.22	−0.14	−0.07	−0.01	0.05	0.10	0.14
	Function (11) $x = 1 - 0.4432 * [(1 + r)^{50} - 1]/[r * (1 + r)^{50}]$									
r	1%	2%	3%	4%	5%	6%	7%	8%	9%	10%
x	−14.70	−11.59	−9.31	−7,61	−6.31	−5.31	−4.53	−3.90	−3.39	2.97
r	11%	12%	13%	14%	15%	16%	17%	18%	19%	20%
x	−2.62	−2.33	−2.07	−1.86	−1.67	−1.50	−1.36	−1.22	−1.11	−1.00
	Function (12) $x = 1 - 0.2931 * [(1 + r)^{50} - 1]/[r * (1 + r)^{50}]$									
r	1%	2%	3%	4%	5%	6%	7%	8%	9%	10%
x	−9,74	7.61	−6.05	−4.88	−4.00	−3.32	−2.78	−2.35	−2.00	−1.72
r	11%	12%	13%	14%	15%	16%	17%	18%	19%	20%
x	−1.48	−1.27	−1.10	−0.95	−0.82	−0.71	−0.61	−0.52	−0.44	−0.37

	Function (13) $x = 1 - 0.1835 * [(1 + r)^{50} - 1]/[r * (1 + r)^{50}]$									
r	1%	2%	3%	4%	5%	6%	7%	8%	9%	10%
x	−5.88	−4.51	−3.52	−2.77	−2.20	−1.77	−1.42	−1.15	−0.92	−0.74
r	11%	12%	13%	14%	15%	16%	17%	18%	19%	20%
x	−0.59	−0.46	−0.35	−0.25	−0.17	−0.10	−0.03	−0.02	0.08	0.12
	Function (14) $x = 1 - 0.2211 * [(1 + r)^{50} - 1]/[r * (1 + r)^{50}]$									
r	1%	2%	3%	4%	5%	6%	7%	8%	9%	10%
x	−7.43	−5.76	−4.53	−3.62	−2.93	−2.39	−1.97	−1.63	−1.36	−1.13
r	11%	12%	13%	14%	15%	16%	17%	18%	19%	20%
x	−0.94	−0.79	−0.65	−0.53	−0.43	−0.34	−0.26	−0.19	−0.13	−0.08
	Function (15) $x = 1 - 0.2938 * [(1 + r)^{50} - 1]/[r * (1 + r)^{50}]$									
r	1%	2%	3%	4%	5%	6%	7%	8%	9%	10%
x	−9.93	−7.76	−6.17	−4.99	−4.09	−3.39	−2.85	−2.41	−2.06	−1.76
r	11%	12%	13%	14%	15%	16%	17%	18%	19%	20%
x	−1.52	−1.31	−1.14	−0.99	−0.86	−0.74	−0.64	−0.55	−0.47	−0.39
	Function (16) $x = 1 - 0.4928 * [(1 + r)^{50} - 1]/[r * (1 + r)^{50}]$									
r	1%	2%	3%	4%	5%	6%	7%	8%	9%	10%
x	−14.63	−11.53	−9.26	−7.57	−6.28	−5.29	−4.50	−3.88	−3.37	−2.95
r	11%	12%	13%	14%	15%	16%	17%	18%	19%	20%
x	−2.61	−2.31	−2.06	−1.84	−1.66	−1.49	−1.34	−1.21	−1.10	−0.99
	Function (17) $x = 1 - 0.2001 * [(1 + r)^{50} - 1]/[r * (1 + r)^{50}]$									
r	1%	2%	3%	4%	5%	6%	7%	8%	9%	10%
x	−5.90	−4.53	−3.53	−2.78	−2.21	−1.78	−1.43	−1.15	−0.93	−0.75
r	11%	12%	13%	14%	15%	16%	17%	18%	19%	20%
x	−0.59	−0.46	−0.35	−0.26	−0.17	−0.10	−0.04	0.02	0.07	0.12

6.6. Summary of this Chapter

This chapter studies the impact of changes on building carbon dioxide emissions from three aspects: exterior walls, roofs, and exterior windows. Analyze the impact of individual changes in exterior walls on building carbon dioxide emissions in severe cold regions, the impact of individual changes in exterior windows on building carbon dioxide emissions in severe cold regions, and the impact of individual changes in roofs on building carbon dioxide emissions in severe cold regions. DesignBuilder software was used to simulate the impact of simultaneous changes in the three factors of exterior walls, exterior windows, and roofs on building carbon dioxide emissions, and the optimal design plans for Changchun, Shenyang, and Datong were selected based on the orthogonal analysis method.

7.Summary and Prospect

7.1. Summary

This article uses Design Builder modeling software to construct a virtual residential building model and places the model in three locations in Changchun City, Jilin Province, Shenyang City, Liaoning Province, and Datong City, Shanxi Province, in severe cold regions, to simulate and measure annual carbon emissions. Based on changes in building materials and external structural performance changes as the main variable parameters, a comparative analysis of carbon dioxide emissions was conducted. The main conclusions drawn are as follows:

(1) In the past 20 years, the annual average temperature and the average temperature in spring, summer, autumn and winter in Changchun City, Shenyang City and Datong City have shown an upward trend and have shown a multi-fluctuation trend.

(2) The annual average temperature trend rate in Changchun City shows an upward trend, with an average annual increase of 0.023°C. The climate trend rate of annual mean temperature change is 0.23℃/10a. The annual average temperature trend rate in Shenyang City shows an upward trend, with an average annual increase of 0.023℃, and the annual average temperature change climate trend rate is 0.23℃/10a. The annual average temperature trend rate in Datong City shows an upward trend, with an average annual increase of 0.027°C. The climate trend rate of annual mean temperature change is 0.27℃/10a.

(3) The average spring temperature trend rate in Changchun City shows an upward trend, with an average annual increase of 0.038°C. The climate trend rate of spring average temperature change is 0.38℃/10a. The average spring temperature trend rate in Shenyang City shows an upward trend, with an average annual increase of 0.044°C. The climate trend rate of spring average temperature change is 0.44℃/10a. The average spring temperature trend rate in Datong City shows an upward trend, with an average annual increase of 0.058°C. The climate trend rate of spring average temperature change is 0.58℃/10a.

(4) The average summer temperature trend rate in Changchun City shows an upward trend, with an average annual increase of 0.021°C. The

climate tendency rate of summer average temperature change is 0.21℃/10a. The average summer temperature trend rate in Shenyang City shows an upward trend, with an average annual increase of 0.040°C. The climate trend rate of summer average temperature change is 0.40℃/10a. The average summer temperature trend rate in Datong City shows an upward trend, with an average annual increase of 0.016°C. The climate trend rate of summer average temperature change is 0.16℃/10a.

(5) The average autumn temperature trend rate in Changchun City shows an upward trend, with an average annual increase of 0.023°C. The climate tendency rate of autumn average temperature change is 0.23℃/10a. The average temperature trend rate of autumn in Shenyang City shows an upward trend, with an average annual increase of 0.012°C. The climate trend rate of autumn average temperature change is 0.12℃/10a. The average temperature trend rate of autumn in Datong City shows an upward trend, with an average annual increase of 0.012°C. The climate trend rate of autumn average temperature change is 0.12℃/10a.

(6) The average winter temperature in Changchun City shows a slight downward trend, with an average annual decrease of 0.001°C. The climate tendency rate of winter average temperature change is 0.01 ℃/10a. The average winter temperature in Shenyang City shows an upward trend, with an average annual increase of 0.046°C. The climate trend rate of winter average temperature change is 0.46℃/10a. The average winter temperature trend rate in Datong City shows an upward trend, with an average annual increase of 0.054°C. The climate trend rate of winter average temperature change is 0.54℃/10a.

(7) As the temperature changes, the annual carbon dioxide emission trend rate in Datong City, Shenyang City, and Changchun City shows an upward trend. Among them, the average annual carbon dioxide emissions in Changchun City increased by 0.039 tons. The annual carbon dioxide emissions trend rate is 0.38t/10a (passes the significance test of 0.05). The average annual carbon dioxide emissions in Shenyang increased by 0.28 tons. The annual carbon dioxide emission trend rate is 2.8t/10a. The average annual carbon dioxide emissions in Datong City increased by 0.11 tons, and the annual carbon dioxide emissions trend rate was 1.1t/10a.

(8) The spring carbon dioxide emission tendency rate in Changchun City, Shenyang City, and Datong City shows an upward trend with temperature

changes. Among them, Changchun City's spring carbon dioxide emissions increased by 0.17 tons, and the spring carbon dioxide emission tendency rate was 1.7t/10a. Shenyang's spring carbon dioxide emissions increased by 0.12 tons year-on-year, and the spring carbon dioxide emission tendency rate was 1.2t/10a. Datong City's spring carbon dioxide emissions increased by 0.051 tons, and the spring carbon dioxide emission tendency rate was 0.51t/10a.

(9) The summer carbon dioxide emission tendency rate in Changchun City, Shenyang City, and Datong City shows an increasing trend with changes in temperature. Changchun City's summer carbon dioxide emissions increased by 0.01 *t*, and the summer carbon dioxide emission tendency rate was 0.06t/10a. Shenyang's annual summer carbon dioxide emissions increase by 0.03 *t*, and the summer carbon dioxide emission trend rate is 0.28t/10a. The summer carbon dioxide emission in Datong City increased by 0.065 *t*, and the summer carbon dioxide emission tendency rate was 0.65t/10a.

(10) The tendency rate of carbon dioxide emissions in Changchun, Shenyang and Datong cities in autumn shows an increasing trend with temperature changes. Among them, Changchun City's autumn carbon dioxide emissions increased by 0.03 *t*, and the autumn carbon dioxide emission trend rate was 0.3t/10a. Shenyang City's carbon dioxide emissions increase by 0.018*t* every autumn, and the autumn carbon emission trend rate is 0.18t/10a. The CO_2 emission in Datong City increased by 0.005*t* in autumn, and the tendency rate of CO_2 emission in autumn was 0.05t/10a.

(11) Changchun City, Shenyang City, and Datong City show an increasing trend in winter carbon dioxide emission tendency with temperature changes. Changchun City's winter carbon dioxide emissions increased by 0.018t, and the winter carbon dioxide emission tendency rate was 0.18t/10a. Shenyang's winter carbon dioxide emissions increased by 0.087t, and the winter carbon dioxide emissions trend rate was 0.87t/10a. The CO_2 emission in Datong City increased by 0.29t in winter, and the CO_2 emission trend rate in winter was 2.9t/10a.

(12) Compared with the life cycle carbon emissions of the original structure buildings in Changchun City, the life cycle carbon emissions of the wooden structure buildings were reduced by 1898.26 tCO_2e, and the life cycle carbon emissions of the wooden structure buildings were reduced by 30.8%. Compared with the life cycle carbon emissions of the original structural buildings in Shenyang City, the life cycle carbon emissions of wooden

structure buildings have been reduced by 1598.26 tCO_2e, and the life cycle carbon emissions of wooden structure buildings have been reduced by 28.5%. Compared with the life cycle carbon emissions of the original structural buildings in Datong City, the life cycle carbon emissions of wooden structure buildings have been reduced by 1634.76 tCO_2e, and the life cycle carbon emissions of wooden structure buildings have been reduced by 30.5%.

(13) From the perspective of the building envelope, base on the perspective of carbon dioxide emissions, the best parameter design options for this project are 85*mm* thick EPS polystyrene foam board for the exterior wall, 100*mm* thick EPS polystyrene foam board for the roof, plastic steel frame and triple-glazed windows 6+Vacuum+6 double silver Low-e+PolyVinyl Butyral Film+6. The implementation of the plan in Changchun City will lead to a reduction of carbon dioxide emissions by 21.26%, the implementation of the plan in Shenyang City will lead to a reduction of 12.34% in carbon dioxide emissions, and the implementation of the plan in Datong City will lead to a reduction of 14.99% in carbon dioxide emissions.

(14) Since the average temperature is rising year by year, the building carbon emission are also rising year by year. At the same time, due to the extreme weather, the carbon emissions required for summer cooling and winter heating are increasing year by year. China faces a severe situation in achieving the goals of carbon peak in 2030 and carbon neutrality in 2060. Therefore, the optimal design plan recommended in this article at this stage is based on the carbon emission reduction effect.

(15) This article provides an important basis for the selection of design plans of residential buildings in severe cold regions. Provide environmental design methods for carbon emission reduction of residential buildings in severe cold regions to help China achieve carbon neutrality in 2060.

7.2. Prospect

(1) This article only analyzes temperature in the past 20 years, and the analysis time range should be expanded in the future.

(2) Based on the conclusions of this article, for the emission reduction design of residential buildings in severe cold regions, it is recommended to modify the exterior walls, exterior windows, and roofs at the same time. But it

should be adjusted according to the actual situation.

(3) Since the design methods and design materials mentioned in this article are limited and cannot represent all design solutions, more solutions can be analyzed later.

(4) This article only selects improvement plans for materials that are currently widely used in the market. The application of new materials can be tried in the future.

(5) New building materials with lower prices can be developed to improve the emission reduction rate.

(6) This article only simulates and analyzes the geographical environment of Changchun City in Jilin Province, Shenyang City in Liaoning Province, and Datong City in Shanxi Province in severe cold regions. Simulation analysis of residential buildings in more severe cold regions can be carried out in the future.

(7) The results of this article will change depending on the selected reference region and reference citation data. If you use this research method, please select the latest parameters according to legal regulations and select the applicable region.

Reference

[1] United Nations Framework Convention on Climate Change. “The Paris Agreement.” United Nations Climate Change, United Nations, 2015, unfccc.int/process-and-meetings/the-paris-agreement.

[2] Center (APRC), Asia and Pacific Research. “Latest IPCC Report Presses the World to “Halve CO_2 Emissions by 2030” — UN Secretary General Warns That “the Climate Time Bomb Is Ticking.”” ScienceJapan, sj.jst.go.jp/stories/2023/s0522-01p.html.

[3] Global Carbon Project. “Global Carbon Project (GCP).” Globalcarbonproject.org, Global Carbon Project (GCP), 2019, www.globalcarbonproject.org/.

[4] China Building Energy Conservation Association.China Energy Transition Status Report, China Construction Industry Press: Chongqing, 2020.

[5] China Building Energy Conservation Association. Series of Research Reports on Carbon Emissions in China’s Urban and Rural Construction Fieldst , China Construction Industry Press: Chongqing, 2022.

[6] Chuai, Xiaowei, et al. “China’s Construction Industry-Linked Economy-Resources-Environment Flow in International Trade.” Journal of Cleaner Production, vol. 278, Jan. 2021, p. 123990, https://doi.org/10.1016/j.jclepro.2020.123990.

[7] Rao, Congjun, et al. “Energy Demand Forecasting in China: A Support Vector Regression-Compositional Data Second Exponential Smoothing Model.” Energy, Nov. 2022, p. 125955, https://doi.org/10.1016/j.energy.2022.125955.

[8] Hong, Lixuan, et al. “Building Stock Dynamics and Its Impacts on Materials and Energy Demand in China.” Energy Policy, vol. 94, July 2016, pp. 47–55, https://doi.org/10.1016/j.enpol.2016.03.024. Accessed 28 Mar. 2022.

[9] China’s Policy Strategies for Green Low-Carbon Development: Perspective from South-South Cooperation .

[10] International Energy Agency. “Global CO_2 Emissions Rebounded to Their Highest Level in History in 2021 - News.” IEA, IEA, 8 Mar.2022,www.iea.org/news/global-CO_2-emissions-rebounded-to-their-highest-level-in-history-in-2021.

[11] International Energy Agency. “CO_2 Emissions in 2022 – Analysis.” IEA,

Mar. 2023, www.iea.org/reports/CO_2-emissions-in-2022.

[12] Xu, Li, et al. "Driving Forces of Carbon Dioxide Emissions in China's Cities: An Empirical Analysis Based on the Geodetector Method." Journal of Cleaner Production, vol. 287, Mar. 2021, p. 125169, https://doi.org/10.1016/j.jclepro.2020.125169.

[13] Masson-Delmotte, Valérie, et al. Global Warming of 1.5°c an IPCC Special Report on the Impacts of Global Warming of 1.5°c above Pre-Industrial Levels and Related Global Greenhouse Gas Emission Pathways, in the Context of Strengthening the Global Response to the Threat of Climate Change, Sustainable Development, and Efforts to Eradicate Poverty Edited by Science Officer Science Assistant Graphics Officer. 2018.

[14] "NewEnergyNews: TODAY'S STUDY: DOING EE the CHINESE WAY."Newenergynews.blogspot.com,newenergynews.blogspot.com/2012/07/todays-study-doing-ee-chinese-way.html. Accessed 19 Dec. 2023.

[15] Lang, Siwei. "Progress in Energy-Efficiency Standards for Residential Buildings in China." Energy and Buildings, vol. 36, no. 12, Dec. 2004, pp. 1191–1196, https://doi.org/10.1016/j.enbuild.2003.09.014. Accessed 8 May 2019.

[16] Zhang, Ying, et al. "A Review of Green Building Development in China from the Perspective of Energy Saving." Energies, vol. 11, no. 2, 2 Feb. 2018, p. 334, https://doi.org/10.3390/en11020334.

[17] "The 10th Five-Year Plan for Energy Conservation and Resources Comprehensive Utilization."English.mee.gov.cn,english.mee.gov.cn/Resources/Plans/Special_Fiveyear_Plan/200709/t20070910_108975.shtml.

[18] "12thFiveYearPlan."English.www.gov.cn,English.www.gov.cn/12thFiveYearPlan

[19] Li Jintang, Sun Zongyu, Li Ji, Wang Fei, Zuo Xu, Hou Yuebin, Ma Mengru, Qiao Biao, Feng Xiaomei, Wang Xuan. Research on clean heating and energy-saving renovation projects of typical existing residential buildings and rural houses. Construction Technology, 2020 (02): 26- 30+35.

[20] He Zhangjin. Analysis of influencing factors and benefit evaluation of green building energy conservation in Hubei region. Wuhan Light Industry University Science, 2017.

[21] Wang Yilin, Deng Qinqin, Li Deying. Energy-saving optimization of existing residential building envelope renovation in cold areas Research. New Building Materials, 2019,46(12):145-148+152.

[22] Ren Jingwei. Research on factors affecting energy consumption and indoor comfort of existing residences in cold areas. Dalian University of Technology, 2018.

[23] “Welcome to CASBEE Website!!”Www.ibec.or.jp, www.ibec.or.jp/CASBEE/english/.

[24] Wang, Qian, et al. “Exploring the Influences of Green Industrial Building on the Energy Consumption of Industrial Enterprises: A Case Study of Chinese Cigarette Manufactures.” Journal of Cleaner Production, vol. 231, Sept. 2019, pp. 370–385, https://doi.org/10.1016/j.jclepro.2019.05.136. Accessed 1 Dec. 2021.

[25] “Carbon Neutrality | Global Issues - JapanGov -.” JapanGov, www.japan.go.jp/global_issues/carbon_neutrality/index.html.

[26] “France Energy Efficiency & Trends Policies | France Profile | ODYSSEE-MURE.”www.odyssee-Mure.eu,www.odyssee-mure.eu/publications/efficiency-trends-policies-profiles/france.html.

[27] “Doubling Global Pace of Energy Efficiency Progress by 2030 Is Key Step in Efforts to Reach Net Zero Emissions - News.” IEA, www.iea.org/news/doubling-global-pace-of-energy-efficiency-progress-by-2030-is-key-step-in-efforts-to-reach-net-zero-emissions.

[28] Ang, Tze-Zhang, et al. “A Comprehensive Study of Renewable Energy Sources: Classifications, Challenges and Suggestions.” Energy Strategy Reviews, vol. 43, Sept. 2022, p. 100939, https://doi.org/10.1016/j.esr.2022.100939.

[29] Ömer KAYNAKLI, Kaynakli F . Determination Of Optimum Thermal Insulation Thickness For External Walls Considering The Heating, Cooling And Annual Energy Requirements[J]. Uludağ University Journal of the Faculty of Engineering, 2016, 21(1):229.37

[30] Ucar A , Lnalli M , Balo F . Application of Three Different Methods for Determination of Optimum Insulation Thickness in External Walls[J]. Environmental progress, 2011, 30(4):p.709-719.

[31] Ashouri M, Astaraei F R, Ghasempour R, et al. Optimum insulation thickness determination of a building wall using exergetic life cycle assessment[. Applied Thermal Engineering, 2016:S1359431116308699.

[32] Sisman N , Kahya E , Aras N , et al. Determination of optimum insulation thickness of the external walls and roof (ceiling) for Turkey different degree-day regions. Energy Policy, 2007, 35(10): 5151-5155.

[33] Carletti, Cristina, Sciurpi, Fabio, Pierangioli, Leone. The Energy

Upgrading of Existing Buildings: Window and Shading Device Typologies for Energy Efficiency Refurbishment. Sustainability, 6(8):5354-537.

[34] Cascone S, Catania F, Gagliano A, et al. A comprehensive study on green roof performance for retrofitting existing buildings. Building and Environment, 2018, 136(MAY): 227-239.

[35] Berardinis P D, Rotilio M, Capannolo L. Energy and Sustainable Strategies in the Renovation of Existing Buildings: An Italian Case Study. Sustainability, 2017, 9(8).

[36] IEA. "An Energy Sector Roadmap to Carbon Neutrality in China – Analysis." IEA, Sept. 2021, www.iea.org/reports/an-energy-sector-roadmap-to-carbon-neutrality-in-china.

[37] Liu, Nieyangzi, et al. "Road Life-Cycle Carbon Dioxide Emissions and Emission Reduction Technologies: A Review." Journal of Traffic and Transportation Engineering (English Edition), vol. 9, no. 4, 1 Aug. 2022, pp. 532–555, www.sciencedirect.com/science/article/pii/S2095756422000587, https://doi.org/10.1016/j.jtte.2022.06.001.

[38] Ali, Khozema Ahmed , et al. "Issues, Impacts, and Mitigations of Carbon Dioxide Emissions in the Building Sector." Sustainability, vol. 12, no. 18, 10 Sept. 2020, p. 7427. MDPI, www.mdpi.com/2071-1050/12/18/7427, https://doi.org/10.3390/su12187427.

[39] Yang, Han, et al. "Research on Carbon Reduction of Residential Buildings in Severe Cold Regions Based on Renovation of Envelopes." Energies, vol. 15, no. 5, 1 Jan. 2022, p. 1873, www.mdpi.com/1996-1073/15/5/1873, https://doi.org/10.3390/en15051873. Accessed 17 Dec. 2023.

[40] Yang, Han, et al. "Research on the Whole Lifecycle Emission Reduction Effect of Buildings with Different Structures in Severely Cold Regions—a Case Study in China." Energies, vol. 16, no. 14, 1 Jan. 2023, p. 5285,www.mdpi.com/1996-1073/16/14/5285,https://doi.org/10.3390/en16145285. Accessed 17 Dec. 2023.

[41] Flower, David J. M., and Jay G. Sanjayan. "Green House Gas Emissions due to Concrete Manufacture." The International Journal of Life Cycle Assessment, vol. 12, no. 5, 2 May 2007, pp. 282–288, https://doi.org/10.1065/lca2007.05.327.

[42] Min, Ji, et al. "The Effect of Carbon Dioxide Emissions on the Building Energy Efficiency." Fuel, vol. 326, 15 Oct. 2022, p. 124842, www.sciencedirect.com/science/article/pii/S0016236122016854#b0520,

https://doi.org/10.1016/j.fuel.2022.124842.

[43] Ramage, Michael H., et al. “The Wood from the Trees: The Use of Timber in Construction.” Renewable and Sustainable Energy Reviews, vol. 68, no. 1, Feb. 2017, pp. 333–359. sciencedirect, www.sciencedirect.com/science/article/pii/S1364032116306050, https://doi.org/10.1016/j.rser.2016.09.107.

[44] Adesina, Adeyemi. “Recent Advances in the Concrete Industry to Reduce Its Carbon Dioxide Emissions.” Environmental Challenges, vol. 1, Dec. 2020, p. 100004, https://doi.org/10.1016/j.envc.2020.100004.

[45] Habert, G., et al. “Environmental Impacts and Decarbonization Strategies in the Cement and Concrete Industries.” Nature Reviews Earth & Environment, vol. 1, no. 11, 1 Nov. 2020, pp. 559–573,www.nature.com/articles/s43017-020-0093-3,https://doi.org/10.1038/s43017-020-0093-3.

[46] Costa, F.N., and D.V. Ribeiro. “Reduction in CO_2 Emissions during Production of Cement, with Partial Replacement of Traditional Raw Materials by Civil Construction Waste (CCW).” Journal of Cleaner Production, vol. 276, Dec. 2020, p. 123302, https://doi.org/10.1016/j.jclepro.2020.123302. Accessed 4 Nov. 2020.

[47] Purnell, P. “Material Nature versus Structural Nurture: The Embodied Carbon of Fundamental Structural Elements.” Environmental Science & Technology, vol. 46, no. 1, 5 Dec. 2011, pp. 454–461, https://doi.org/10.1021/es202190r.

[48] Miller, Sabbie A., et al. “Carbon Dioxide Reduction Potential in the Global Cement Industry by 2050.” Cement and Concrete Research, vol. 114, Dec. 2018, pp. 115–124, https://doi.org/10.1016/j.cemconres.2017.08.026.

[49] Moon, Eun-Jin, and Young Cheol Choi. “Carbon Dioxide Fixation via Accelerated Carbonation of Cement-Based Materials: Potential for Construction Materials Applications.” Construction and Building Materials, vol. 199, Feb. 2019, pp. 676–687, https://doi.org/10.1016/j.conbuildmat.2018.12.078. Accessed 23 Nov. 2019.

[50] Strzałkowski, Jarosław, et al. “Thermal Performance of Building Envelopes with Structural Layers of the Same Density: Lightweight Aggregate Concrete versus Foamed Concrete.” Building and Environment, vol. 196, June 2021, p. 107799, https://doi.org/10.1016/j.buildenv.2021.107799. Accessed 28 Mar. 2021.

[51] “EnergyPlus - an Overview | ScienceDirect Topics.” Www.sciencedirect.com,www.sciencedirect.com/topics/engineering/energy

plus.,

[52] Hafez, Fatma S., et al. “Energy Efficiency in Sustainable Buildings: A Systematic Review with Taxonomy, Challenges, Motivations, Methodological Aspects, Recommendations, and Pathways for Future Research.” Energy Strategy Reviews, vol. 45, no. 101013, Jan. 2023, p. 101013, www.sciencedirect.com/science/article/pii/S2211467X22002073.

[53] Patterson, Paul G., and Tasman Smith. “A Cross-Cultural Study of Switching Barriers and Propensity to Stay with Service Providers.” Journal of Retailing, vol. 79, no. 2, Jan. 2003, pp. 107–120, https://doi.org/10.1016/s0022-4359(03)00009-5. Accessed 29 Apr. 2020.

[54] “Net Present Value - an Overview | ScienceDirect Topics.” Www.sciencedirect.com,www.sciencedirect.com/topics/social-sciences/net-present-value.

[55] Cui, Lian-Biao, et al. “How Will the Emissions Trading Scheme Save Cost for Achieving China’s 2020 Carbon Intensity Reduction Target?” Applied Energy, vol. 136, Dec. 2014, pp. 1043–1052, https://doi.org/10.1016/j.apenergy.2014.05.021. Accessed 16 Aug. 2020.

[56] “Payback Time - an Overview | ScienceDirect Topics.” Www.sciencedirect.com,www.sciencedirect.com/topics/engineering/payback-time.

[57] “Simple Payback Time - an Overview | ScienceDirect Topics.” www.sciencedirect.com,www.sciencedirect.com/topics/engineering/simple-payback-time.

[58] Zhou, Wen-Jie, et al. “Modelling of Ventilation and Dust Control Effects during Tunnel Construction.” International Journal of Mechanical Sciences, vol. 160, 1 Sept. 2019, pp. 358–371, https://doi.org/10.1016/j.ijmecsci.2019.06.037. Accessed 23 Apr. 2023.

[59] Ouyang, Qi, et al. “Monthly Rainfall Forecasting Using EEMD-SVR Based on Phase-Space Reconstruction.” Water Resources Management, vol. 30, no. 7, 17 Mar. 2016, pp. 2311–2325, https://doi.org/10.1007/s11269-016-1288-8. Accessed 10 Dec. 2020.

[60] Chang, Qing, et al. “Association between Air Pollutants and Outpatient and Emergency Hospital Visits for Childhood Asthma in Shenyang City of China.” International Journal of Biometeorology, vol. 64, no. 9, 9 May 2020, pp. 1539–1548, https://doi.org/10.1007/s00484-020-01934-9. Accessed 27 Aug. 2020.

[61] “Landscape Ecological Effect Analysis of Land Use Change in Datong City Using Remote Sensing | IEEE Conference Publication | IEEE Xplore.”

Ieeexplore.ieee.org,ieeexplore.ieee.org/abstract/document/5137627.Accessed 19 Dec. 2023.

[62] "Announcement of the Ministry of Housing and Urban-Rural Development on the release of the industry standard "Energy-saving Design Standard for Residential Buildings in Severe and Cold Areas." Www.mohurd.gov.cn,www.mohurd.gov.cn/gongkai/zhengce/zhengcefilelib/201909/20190910_241751. html.Accessed 14 May 2024.

[63] "Announcement of the Ministry of Housing and Urban-Rural Development on the release of the national standard "Timber Structure Design Standards"."Www.mohurd.gov.cn,www.mohurd.gov.cn/gongkai/zhengce/zhengcefilelib/201806/20180626_236549.html. Accessed 14 May 2024.

[64] "Announcement of the Ministry of Housing and Urban-Rural Development on the release of the national standard "Building Carbon Emission Calculation Standard."www.mohurd.gov.cn,www.mohurd.gov.cn/gongkai/zhengce/zhengcefilelib/201905/20190530_240723.html.

[65] He Jiongying, et al. "Review and Prospects of Forestry Carbon Sink Accounting Research. | Issues of Forestry Economics | EBSCOhost." Openurl.ebsco.com, 1 Sept. 2021, openurl.ebsco.comAccessed 14 May 2024.

[66] Yu Luji, et al. "Spatial and temporal characteristics of forest carbon sink value in Henan Province and its influencing factors." Stbctb.cnjournals.com, 25 Oct. 2023, stbctb.cnjournals.com/html/2023/5/20230534.htm. Accessed 14 May 2024.

[67] Zhuang Qihua, et al. "Research on forest carbon sink accounting measurement model. | Issues of Forestry Economics | EBSCOhost. ” Openurl.ebsco.com, 1 July 2022, openurl.ebsco.com

[68] Xu Wenqi, and Chao Wang. "Analysis of energy-saving building design in construction engineering design." Modern Engineering Project Management, vol. 2, no. 9, 10 July 2023, pp. 161–163, ojs.omniscient.sg/index.php /mepm/article/view/18491.

[69] Zhang Xudong. "A brief analysis of building energy consumption analysis and energy-saving measures." Urbanization and Land Use, vol. 11, 6 June 2023, p. 72, www.hanspub.org/journal/PaperInformation?PaperID=67315&, https://doi.org/10.12677/ULU.2023.112011.

[70] Zhao Quanbin, et al. "Research progress on connection nodes of autoclaved aerated concrete exterior wall panels. | New Building Materials

/ Xinxing Jianzhu Cailiao | EBSCOhost." Openurl.ebsco.com, 1 Apr. 2023, openurl.ebsco.com/EPDB %3Agcd%3A2%3A11106098/detailv2?sid=ebsco%3Aplink%3Ascholar&id=ebsco%3Agcd%3A163624782&crl=c.

[71] "Residential Design Code [With Provisions] GB50096-2011 Construction Standard Database.www.jianbiaoku.com,www.jianbiaoku.com/webarbs/book/407/1348650.shtml. Accessed 15 May 2024.

[72] "Announcement of the Ministry of Housing and Urban-Rural Development on the release of the national standard "General Specifications for Building Energy Saving and Renewable Energy Utilization"."www.mohurd.gov.cn,www.mohurd.gov.cn/gongkai/zhengce/zhengcefilelib/202110/20211013_762460 .html.

[73] General Atlas "Energy-Saving Doors and Windows"_General Atlas_Beijing Municipal Planning and Natural Resources Commission." Ghzrzyw.beijing.gov.cn,ghzrzyw.beijing.gov.cn/biaozhunguanli/bzgj/tytj/202305/t20230504_3085843.html. Accessed 16 May 2024.

[74] "Photothermal Performance of Glass Curtain Walls" GB/T 18091-2015_SOSOARCH."www.sosoarch.com,www.sosoarch.com/guifan/details.aspx?id=1227.

[75] "Notice on the public solicitation of opinions on the "Enterprise Greenhouse Gas Emissions Accounting Methods and Reporting Guidelines for Power Generation Facilities" and "Enterprise Greenhouse Gas Emission Verification Technical Guidelines for Power Generation Facilities"." Www.mee.gov.cn,www.mee.gov.cn/xxgk2018/xxgk/xxgk06/202211/t20221109_1004058.html. Accessed 16 May 2024.

[76] "Cumulative trading volume of carbon emission quotas reaches 179 million tons_Rolling News_China Government Network." Www.gov.cn, www.gov.cn/xinwen/2022-01/04/content_5666282.htm. Accessed 16 May 2024.

[77] "Interim Regulations on the Management of Carbon Emissions Trading (Order No. 775 of the State Council of the People's Republic of China)."www.mee.gov.cn,www.mee.gov.cn/zcwj/gwywj/202402/t20240205_1065850.shtml. Accessed 16 May 2024 .

[78] "2022 Jilin Statistical Yearbook." Tjj.jl.gov.cn, tjj.jl.gov.cn/tjsj/tjnj/2022/ml/indexc.htm.

[79] "Liaoning Provincial Bureau of Statistics." Tjj.ln.gov.cn, tjj.ln.gov.cn/. Accessed 16 May 2024.

[80] "Shanxi Survey Team of the National Bureau of Statistics."

Sxzd.stats.gov.cn, sxzd.stats.gov.cn/. Accessed 16 May 2024.